bioRxiv preprint doi: https://doi.org/10.1101/2025.02.09.637280; this version posted February 10, 2025. The copyright holder for this preprint (which was not certified by peer review) is the author/funder, who has granted bioRxiv a license to display the preprint in perpetuity. It is made available under a CC-BY-NC-ND 4.0 International license.

Neofunctionalized RGF pathways drive haustorial organogenesis in parasitic plants

Maxwell R. Fishman[1], Anne Greifenhagen[1], Takanori Wakatake[1†], Anuphon Laohavisit[1‡], Ryoko Hiroyama[1], Sachiko Masuda[1], Arisa Shibata[1], Satoko Yoshida[2], Ken Shirasu[1,3,*]

1. RIKEN Center for Sustainable Resource Science, RIKEN-TRIP, Yokohama, Kanagawa, Japan

2. Graduate school of Science and Technology, Graduate School of Science and Technology, Ikoma, Nara, Japan

3. Graduate School of Science, The University of Tokyo, Hongo, Bunkyo, Tokyo, Japan

†Current address: Nara Institute of Science and Technology, Graduate School of Science and Technology, Ikoma, Nara, Japan

‡Current address: Institute of Transformative Bio-Molecules, Nagoya, Japan

*Corresponding author: Ken Shirasu, ken.shirasu@riken.jp

Abstract

Parasitic plants initiate rapid *de novo* organogenesis of a specialized feeding structure called a haustorium upon contact with their hosts. Currently, little is known about the internal signals regulating haustorium development. Here, we identify root meristem growth factor (RGF) peptides in *Phtheirospermum japonicum* as endogenous inducers of prehaustorium formation. Treatment with specific RGF peptides in the absence of hosts triggered prehaustoria and induced

bioRxiv preprint doi: https://doi.org/10.1101/2025.02.09.637280; this version posted February 10, 2025. The copyright holder for this preprint (which was not certified by peer review) is the author/funder, who has granted bioRxiv a license to display the preprint in perpetuity. It is made available under a CC-BY-NC-ND 4.0 International license.

expression of *PjYUC3*, a gene required for auxin biosynthesis and prehaustorium formation. CRISPR-mediated knockouts showed that PjRGFR1 and PjRGFR3, receptors activated by the haustorium specific RGF peptides PjRGF2 and PjRGF5, are essential for prehaustorium formation, revealing functional redundancy. Phylogenic analyses indicate that PjRGF2 is broadly conserved among Orobanchaceae, whereas PjRGF5 appears to have recently evolved through tandem multiplication and neofunctionalization. Our findings establish RGF peptides and their corresponding receptors as critical components of haustorium developmental signaling and provide insights into the evolutionary trajectories that shape plant parasitism.

Teaser: Plant peptide hormones regulate and induce the parasitic plant specialized organ for connecting to and feeding from the host.

Introduction

Parasitism has independently evolved 12 to 13 times from autotrophic angiosperms and has resulted in around 1% of angiosperms being either root or shoot parasites (*1*, *2*). Parasitic plants occur as obligate non-photosynthetic holoparasites or obligate photosynthetic hemiparasites that both require a host to survive or as facultative parasites that can survive without a host (*3*). In order to parasitize hosts, parasitic plants form a direct connection with host plants through a specialized organ called a haustorium (*2*). Haustoria arise *de novo* upon host contact and progress through specific developmental stages, starting with the prehaustorium, followed by the formation of intrusive cells that penetrate the host tissue, and culminating in the establishment of a vascular connection (*2*). This intimate linkage enables parasitic plants to secure water,

bioRxiv preprint doi: https://doi.org/10.1101/2025.02.09.637280; this version posted February 10, 2025. The copyright holder for this preprint (which was not certified by peer review) is the author/funder, who has granted bioRxiv a license to display the preprint in perpetuity. It is made available under a CC-BY-NC-ND 4.0 International license.

minerals, and nutrients from their hosts, a process essential for survival of obligate parasites (*1*–*3*).

The family Orobanchaceae consists predominantly of root parasites (*4*), encompassing agriculturally devastating obligate parasites in the genera *Orobanche*, *Phelipanche*, *Alectra*, and *Striga*, as well as comparatively benign facultative parasites in *Pedicularis* and *Phtheirospermum* (*5*, *6*). Most members of this family initiate prehaustoria formation upon the perception of lignin- and phenolic-based host-derived haustorium-inducing factors (HIFs), even in the absence of a host (*7*, *8*). The first identified HIF was 2,6-dimethoxy-*p*-benzoquinone (DMBQ) (*9*). DMBQ is a lignin-derived quinone that induces prehaustoria in *Striga* and most other hemiparasitic plants in Orobanchaceae (*10*). The obligate holoparasites *Phelipanche* and *Orobanche* develop prehaustoria in response to cytokinins, sphaeropsidones, and very high concentrations of DMBQ (*11*, *12*). DMBQ has become a central tool to dissect the early signaling pathway underlying haustorium development, particularly in the facultative parasites *Phtheirospermum japonicum* and *Triphysaria versicolor,* and in the obligate hemiparasite *Striga hermonthica* (*13*–*17*). DMBQ, and other similar quinone-based HIFs, are first sensed by CARD1-LIKE (CADL) receptor kinases (*14*), triggering Ca^{2+} signaling in roots and activating a MAPK cascade. These early signals result in the differential regulation of hundreds of genes, leading to the accumulation of reactive oxygen species (ROS) and the *de novo* biosynthesis of auxin through the up-regulation of YUCCA3 MONOOXYGENASE (YUC3) specifically at the site of haustorium initiation (*13*, *15*, *18*). Both ROS and auxin are essential for haustorium development; however, the signaling pathways linking the initial CADL signaling cascade to the downstream factors such as YUC3 are largely unknown.

bioRxiv preprint doi: https://doi.org/10.1101/2025.02.09.637280; this version posted February 10, 2025. The copyright holder for this preprint (which was not certified by peer review) is the author/funder, who has granted bioRxiv a license to display the preprint in perpetuity. It is made available under a CC-BY-NC-ND 4.0 International license.

ROOT GROWTH MERISTEM FACTOR (RGF) peptides (also referred to as GLV or CLEL peptides) were initially identified for their role in maintaining the root apical meristem (RAM) in *Arabidopsis thaliana* (from here on referred to as Arabidopsis) but also regulate lateral root elongation and spacing, as well as root gravitropism (*19–22*). They consist of a family of sulfated plant peptide hormones present in all land plants outside of hornworts and mosses (*23*). They serve as ligands for the RGF RECEPTOR (RGFR)/RGF INSENSITIVE (RGI) leucine-rich repeat receptor-like kinases where the conserved tyrosine, proline, and histidine/asparagine in the mature peptide are critical for interacting with RGFRs or their co-receptors (*24–26*). The regulatory role of RGF peptides in maintaining the RAM is partially accomplished by stabilizing the AP2-type transcription factor PLETHORA2 (PLT2) through the production of superoxide radical (O_2^-) (*27*). Moreover, RGF peptides selectively regulate a subset of auxin-responsive genes and mobilize PIN proteins to specify auxin localization (*22*, *28*). Given the importance of auxin and ROS during haustorium development in parasitic plants, RGF peptides are plausible regulators of haustorium signaling.

In this current study we identified three RGF peptides in *P. japonicum* (PjRGFs) that are up-regulated following DMBQ treatment. Treatment of these DMBQ-induced PjRGF peptides led to an up-regulation of *PjYUC3* and induced prehaustoria in *P. japonicum*. Two of these PjRGF peptides are specifically expressed in the prehaustorium, reflecting the localization patterns of a *P. japonicum* PLT2 homologue (PjPLT) and O_2^-. Further analysis of RGF peptides in several Orobanchaceae species uncovered a single conserved haustorium-specific RGF peptide that also induces prehaustoria in *Striga hermonthica*. Genetic analysis further revealed that knockouts of two PjRGFRs reduced the number of DMBQ-induced prehaustoria in *P. japonicum* hairy roots and one PjRGF peptide regulates cell division at the apex of the

bioRxiv preprint doi: https://doi.org/10.1101/2025.02.09.637280; this version posted February 10, 2025. The copyright holder for this preprint (which was not certified by peer review) is the author/funder, who has granted bioRxiv a license to display the preprint in perpetuity. It is made available under a CC-BY-NC-ND 4.0 International license.

prehaustorium. Taken together, we established RGF peptides in Orobanchaceae as endogenous prehaustorium inducers, placing RGF signaling downstream of DMBQ and upstream of *YUC3* in the haustorium development pathway. These data suggest that parasitic plants neofunctionalize the RGF signaling pathway for *de novo* organogenesis, contributing to the evolution of plant parasitism.

Results

RGF peptides are up-regulated during haustorium induction

To identify signaling components activated by DMBQ perception, we analyzed RNA-seq data from *P. japonicum* seedlings. Since subtilase encoding-genes, which code for apoplastic proteases, are important for haustorium development (*29*), we searched for apoplastically-cleavable peptide hormone-encoding genes that were up-regulated in response to DMBQ treatment. From this approach, we identified a gene encoding an RGF peptide, from herein called *PjRGF1*, which was induced following DMBQ treatment (Fig. S1A, B; Supplementary Table S1). Although only four RGF peptide-encoding genes were initially annotated in the *P. japonicum* genome (*30*), additional mapping and annotation revealed another 13 putative *RGF* genes, 9 of which were expressed (Fig. 1A; Fig. S2A-C; Supplemental Table S2).

To determine which of these expressed *PjRGFs* were HIF responsive, RT-qPCR was performed on cDNA from *P. japonicum* roots treated for six hours with either DMBQ or *Nicotiana benthamiana* exudate. These data showed that *PjRGF1*, *PjRGF2*, and *PjRGF5* were up-regulated following DMBQ treatment, whereas only *PjRGF2* and *PjRGF5* were induced by *N. benthamiana* exudate (Fig. 1B). Notably, in *S. hermonthica,* the *RGF2* homolog (*ShRGF2*)

bioRxiv preprint doi: https://doi.org/10.1101/2025.02.09.637280; this version posted February 10, 2025. The copyright holder for this preprint (which was not certified by peer review) is the author/funder, who has granted bioRxiv a license to display the preprint in perpetuity. It is made available under a CC-BY-NC-ND 4.0 International license.

was also up-regulated six hours post DMBQ treatment (Fig. S3A, B), suggesting that RGF peptides may play a conserved role in the haustorium developmental signaling pathway across multiple parasitic species within Orobanchaceae.

RGF peptides induce prehaustoria in parasitic plants

RGF peptides induce a variety of root-related phenotypes in autotrophic plants (*19*, *28*). Here, surprisingly, application of PjRGF1, PjRGF2, or PjRGF5 to *P. japonicum* induced prehaustoria (Fig. 1C, D). Unsulfated PjRGF1 and PjRGF2 peptides showed only a weak effect but unsulfated PjRGF5 possessed prehaustorium induction activity (Fig. 1C). Similarly, ShRGF2 treatment of *S. hermonthica* also induced prehaustoria (Fig. S3C, D). These induced structures were morphologically similar to DMBQ-induced prehaustoria in both *P. japonicum* and *S. hermonthica*, and their induction rate was dose dependent in *P. japonicum* (Fig. 1C, D; Fig. S3C. D; S4A). The overall efficacy of the PjRGF peptide treatments was lower than that of DMBQ and varied among individual peptides. Both PjRGF1 and PjRGF5 reached maximal induction at 2 μM, while PjRGF2 was most effective at 5 nM (Fig. 1C). Higher concentrations of PjRGF2 sometimes resulted in nonspecific cell division in the epidermis and cortex (Fig. S4B). Prehaustorium formation begins with controlled cell division in the transition zone (*7*), so nonspecific cell division likely reduced the number of prehaustoria formed and suggests that *P. japonicum* is particularly sensitive to PjRGF2. Overall, these findings demonstrate that PjRGF1, PjRGF2, PjRGF5, and ShRGF2 act as ligands capable of inducing prehaustoria.

PjYUC3 up-regulation was previously found to be downstream of HIF treatment, functioning as an important component during prehaustorium development (*13*). Consistent with

bioRxiv preprint doi: https://doi.org/10.1101/2025.02.09.637280; this version posted February 10, 2025. The copyright holder for this preprint (which was not certified by peer review) is the author/funder, who has granted bioRxiv a license to display the preprint in perpetuity. It is made available under a CC-BY-NC-ND 4.0 International license.

this observation, treatment of *P. japonicum* roots with PjRGF1, PjRGF2, or PjRGF5 induced *PjYUC3* expression six hours after treatment (Fig. 1E), though to a lesser extent than DMBQ. In keeping with the previous findings that auxin accumulates at the apex of the *P. japonicum* prehaustorium, where *PjYUC3* is expressed (*13*), a DR5 reporter revealed auxin localized in the epidermis at the apex of the prehaustorium upon treatment with PjRGF2 or DMBQ, or upon association with host roots (Fig. 2A). These data suggest that the prehaustorium development pathway triggered by PjRGF peptides converges on PjYUC3 mediated auxin biosynthesis, echoing the pathway induced by classic HIFs.

***PjRGF2* and *PjRGF5* expression localizes to the prehaustorium**

Because RGF peptides typically act close to their site of expression (*31*), we investigated whether *PjRGF1*, *PjRGF2*, or *PjRGF5* were specifically expressed in the prehaustorium following DMBQ treatment. We generated transcriptional reporter lines expressing *3x-Venus* tagged with a nuclear localization sequence (NLS) under the control of each *PjRGF* promoter (*PjRGF1/2/5pro*). At one day post DMBQ treatment and one day post inoculation with a host root, *PjRGF2pro* and *PjRGF5pro* were clearly expressed in the prehaustorium, while *PjRGF1pro* was expressed in the epidermis throughout the root, regardless of prehaustorium formation (Fig. 2B). Prior to prehaustorium formation, *PjRGF2pro* showed no expression, while *PjRGF5pro* was observed in the cortex and stele. Given that *PjRGF2* and *PjRGF5* were up-regulated at six hours post DMBQ treatment (Fig. 1B), we hypothesized that their expression might localize at this early time point to the transition zone where prehaustoria form. Indeed, at six hours post DMBQ treatment, *PjRGF2pro* expression was observed around the transition zone, and *PjRGF5pro*

bioRxiv preprint doi: https://doi.org/10.1101/2025.02.09.637280; this version posted February 10, 2025. The copyright holder for this preprint (which was not certified by peer review) is the author/funder, who has granted bioRxiv a license to display the preprint in perpetuity. It is made available under a CC-BY-NC-ND 4.0 International license.

showed increased expression relative to untreated roots (Fig. S5; Fig. S6). Collectively, these data indicate that PjRGF2 and PjRGF5 are prehaustorium-specific RGF peptides likely contributing to haustorium developmental signaling, while other PjRGF peptides may not play a major role.

PjPLT localizes to the prehaustorium

If RGF peptides indeed influence haustorium development, a recognizable marker of their activity should be detectable in the prehaustorium. In Arabidopsis, RGF peptides induce O_2^- production that then stabilizes PLT2 (*27*). Likewise, O_2^- was previously shown to accumulate in the prehaustoria of *S. hermonthica* (*18*). Consistent with these findings, nitro blue tetrazolium staining showed that O_2^- also accumulated in the prehaustorium of *P. japonicum* (Fig. S7). These observations suggest a PLT transcription factor might be involved in prehaustorium development. Among six predicted PLT homologs in *P. japonicum*, only four contain two AP2 domains characteristic of PLTs (Fig. S8A). The closest homolog to Arabidopsis PLT2 is Pjv1_00021464, which was named *PjPLT* (Fig. S8B). Under its native promoter, mNeonGreen-tagged PjPLT (mNG-PjPLT) localized to the RAM prior to DMBQ treatment or host inoculation (Fig. S9A). At one day post-DMBQ treatment, mNG-PjPLT was observed in the RAM, the transition zone, and the outer cell layers at the apex of the prehaustorium. mNG-PjPLT also localized within the prehaustorium at 1 DPI, shifting to the center of the prehaustorium (Fig. 2C). This pattern appears to be regulated post-translationally, as a transcriptional reporter for *PjPLT* was expressed broadly in the meristem, transition, and elongation zones as well as the developing prehaustorium, both at 1 DPT DMBQ and at 1 DPI (Fig. S9B). Given that PjRGF

bioRxiv preprint doi: https://doi.org/10.1101/2025.02.09.637280; this version posted February 10, 2025. The copyright holder for this preprint (which was not certified by peer review) is the author/funder, who has granted bioRxiv a license to display the preprint in perpetuity. It is made available under a CC-BY-NC-ND 4.0 International license.

peptides induce prehaustoria and RGF peptides stabilize PLT2 in *Arabidopisis*, we anticipated that upon exogenous PjRGF treatment PjPLT would localize similarly to what is observed under DMBQ treatment. Indeed, mNG-PjPLT was present in the prehaustorium following PjRGF2 treatment (Fig. 2C). However, mNG-PjPLT was also found throughout an elongated meristemic zone and in the interior of the prehaustorium (Fig. 2C), diverging slightly from its localization under DMBQ treatment or at 1 DPI. Nevertheless, both DMBQ and PjRGF2 guide mNG-PjPLT into the prehaustorium, indicating that small differences in localization still result in successful prehaustorium formation.

PjRGF5 is a novel RGF peptide that underwent a series of tandem duplication events in *P. japonicum*

RGF peptides commonly function redundantly, so it is unsurprising that *PjRGF2* and *PjRGF5* are both expressed in the prehaustorium. Analysis of a *P. japonicum* genome assembly produced from PacBio Continuous Long Reads revealed a series of tandem duplications of *PjRGF5* across five contigs (Fig. 3A). At least five nearly identical copies of *PjRGF5* and six *PjRGF5* pseudogenes reside in these duplications, all of which are associated with LTR, TIR, and Helitron transposable elements (TE), with *PjRGF5-7, PjRGF5-8,* and *PjRGF5-9* having a TIR TE inserted in the intron. These TEs may have driven the duplication events. In addition, subcloning of *PjRGF5* cDNA uncovered yet another *PjRGF5* duplicate (Fig. S10). Several of the contigs carrying *PjRGF5* duplicates are quite small, indicating a poorly assembled region (Fig. 3A), and suggest further copies might remain unassembled. The sequences of the *PjRGF5* replicates are highly conserved, typically differing by only one or two single nucleotide

bioRxiv preprint doi: https://doi.org/10.1101/2025.02.09.637280; this version posted February 10, 2025. The copyright holder for this preprint (which was not certified by peer review) is the author/funder, who has granted bioRxiv a license to display the preprint in perpetuity. It is made available under a CC-BY-NC-ND 4.0 International license.

polymorphisms (SNPs) in the sequences encoding the non-conserved region of the prepropeptide (Fig. S11A,B). For example, two copies, designated PjRGF5-2a and PjRGF5-2b, are identical. Multiple sequence alignment revealed that three annotated *PjRGF5* promoters (*PjRGF5-1pro*, *PjRGF5-2apro*, and *PjRGF5-2bpro*) are practically identical, while the other promoter, labelled PjRGF5-5pro, shares a high degree of similarity up to 1555 bp upstream of the start codon (Fig. S12). In agreement with these results, spatial expression patterns driven by the *PjRGF5-1pro*, *PjRGF5-2bpro* (Fig. S13), and *PjRGF5-5pro* (Fig. 2B) visualized using 3x Venus-NLS were observed in the same epidermal region of the prehaustorium. These data suggest that multiple duplicated genes together drive the production of bioactive PjRGF5 in the prehaustorium.

The extensive duplication of *PjRGF5* points to a potential importance for haustorium development in *P. japonicum* and possibly other parasitic Orobanchaceae species. A phylogenetic analysis of RGF prepropeptides from *P. japonicum,* six parasitic Orobanchaceae species and two non-parasitic Orobanchaceae species showed that PjRGF1, PjRGF2, and PjRGF5 each occupy distinct clades (Fig. 3B, Supplemental Table S2) (*6*, *32–35*). Surprisingly, the mature peptide for PjRGF1 and PjRGF5 did not align with the other RGF peptides within their clades, while the mature peptide of PjRGF2 was conserved across *Lindenbergia*, *Pedicularis*, and *Striga* (Fig. 3C, Supplemental Table S2). The only exceptions were the obligate holoparasites *Orobanche cumana* and *Phelipanche aegyptiaca,* which lack a PjRGF2 homolog. These data suggest that PjRGF1 and PjRGF5 may be recent acquisitions in *P. japonicum*, while PjRGF2 appears to be a more ancient, conserved haustorium-related RGF peptide in parasitic Orobanchaceae.

Several *PjRGFRs* are expressed in the prehaustorium and PjRGFR1, PjRGFR3, PjRGFR4 are activated by PjRGF2 and PjRGF5

bioRxiv preprint doi: https://doi.org/10.1101/2025.02.09.637280; this version posted February 10, 2025. The copyright holder for this preprint (which was not certified by peer review) is the author/funder, who has granted bioRxiv a license to display the preprint in perpetuity. It is made available under a CC-BY-NC-ND 4.0 International license.

The receptors for RGF peptides, known as RGFRs/RGIs, were first identified in Arabidopsis (*24–26*). Similar to RGF peptides, RGFRs are conserved throughout land plants. A phylogenetic analysis of RGFRs from 360 species reveal three main clades and two sub-clades (Fig. S14) (*6*, *34*, *35*). *P. japonicum* encodes six RGFRs, more than most sequenced parasitic Orobanchaceae species (Supplemental Table S3). RT-qPCR analysis of cDNA extracted from *P. japonicum* root tips six hours post DMBQ or *N. benthamiana* exudate treatments showed that *PjRGFR3* expression decreased significantly only in response to DMBQ treatment and it is possible that *PjRGFR3* downregulation was a response to PjRGF2/5 signaling downstream of HIF perception (Fig. S15). However, spatial expression analysis using *PjRGFR promoter-3x Venus-NLS* reporter lines (*PjRGFRpro*) showed that *PjRGFR3pro* was not expressed in the prehaustorium (Fig. 4A). Instead, *PjRGFR1pro, PjRGFR2pro, PjRGFR4pro* and *PjRGFR5pro* each displayed some haustorium specific expression pattern, particularly when a host root was present, implying that multiple *P. japonicum* RGFRs likely coordinate prehaustorium development.

Given the difference between RT-qPCR data and promoter driven expression patterns, we next assessed which PjRGFRs directly bind to PjRGF2 and PjRGF5. As chimeric LRR-RLK receptors have previously aided in probing ligand-receptor interactions (*36*), we generated PjRGFR-BRI1 chimeras to evaluate their activation by PjRGF2 or PjRGF5 (Fig. S16). A shift in the BES1 transcription factor from its phosphorylated to dephosphorylated state served as a readout of receptor activation. In *N. benthamiana* leaves co-expressing the *PjRGFR-BRI1-HA* variants and *BES1-HA*, treatment with 100 nM PjRGF2 for 30 min activated PjRGFR1-BRI1-HA, PjRGFR3-BRI1-HA, and PjRGFR4-BRI1-HA (Fig 4B), while 100 nM PjRGF5 for 30 min activated PjRGFR3-BRI1-HA, and PjRGFR4-BRI1-HA (Fig 4C). These results suggest that

bioRxiv preprint doi: https://doi.org/10.1101/2025.02.09.637280; this version posted February 10, 2025. The copyright holder for this preprint (which was not certified by peer review) is the author/funder, who has granted bioRxiv a license to display the preprint in perpetuity. It is made available under a CC-BY-NC-ND 4.0 International license.

PjRGFR1, PjRGFR3, and PjRGFR4 function as primary receptors in the prehaustorium signaling cascade of *P. japonicum*.

PjRGFR1 and PjRGFR3 are positive regulators of prehaustorium formation

To determine the role of PjRGF2 and the PjRGFRs responsive to PjRGF2 and PjRGF5, we used the hairy root CRISPR system, a method employed in *P. japonicum* and other plant species with success (*37*, *38*). CRISPR-zCas9i constructs targeting *PjRGF2*, *PjRGFR1*, *PjRGFR3*, and *PjRGFR4*, were generated with a RUBY reporter for transformed roots (Fig. 5A, Fig. S17). The frequency of knockout mutations ranged from 19% to 45% depending on the target gene (Supplemental Tables S4, S5). Transgenic roots expressing RUBY were treated with 10 μM DMBQ for two days, and the presence of prehaustoria was evaluated. Roots were classified as lacking prehaustorium (including minor cell division), displaying a normal prehaustorium, showing aberrant cell division in the prehaustorium, or exhibiting an aborted prehaustorium (Fig. 5A). Only *PjRGFR1* and *PjRGFR3* knockouts significantly reduced the proportion of roots forming prehaustoria compared to the control (Fig. 5B). In contrast, *PjRGFR4* knockouts had no significant effect on DMBQ-induced prehaustorium formation. Interestingly, although *PjRGF2* knockouts did not reduce the number of prehaustoria, they did develop an unusual prehaustorium phenotype more frequently than the control. These abnormal prehaustoria were pointed at the tip rather than rounded like a normal prehaustorium in a way that was reminiscent of an ectopic root (Fig. 5A). However, confocal microscopic images showed that this pointed structure did not resemble a root tip. Rather, it was capped by two large cells that were divided directly at the tip of the abnormal structure (Fig. S18), suggesting *PjRGF2* regulates cell division in the

bioRxiv preprint doi: https://doi.org/10.1101/2025.02.09.637280; this version posted February 10, 2025. The copyright holder for this preprint (which was not certified by peer review) is the author/funder, who has granted bioRxiv a license to display the preprint in perpetuity. It is made available under a CC-BY-NC-ND 4.0 International license.

haustorium. Taken together, these results indicate that two PjRGFRs are crucial for prehaustorium formation and suggest that multiple PjRGF peptides likely function redundantly, given that a PjRGF2 single knockout did not alter number of prehaustoria.

Discussion

Previous insights into the internal signals driving haustorium development beyond the initial HIFs were lacking. Here, we show that RGF peptides function as endogenous signals that positively regulate haustorium formation following DMBQ treatment and are also capable of inducing prehaustoria in *P. japonicum* and *S. hermonthica* in the absence of HIFs. Another recently described endogenous peptide in *P. japonicum*, PjCLE1, can also induce prehaustoria (*39*); however, PjCLE1 is not expressed in the prehaustorium phase and instead shows up later, after xylem bridge formation. In contrast, as expected of peptide hormones involved in prehaustorium development, *PjRGF2* and *PjRGF5* are expressed at early timepoints following HIF perception (Fig. 1B). Peptide hormones often act redundantly, as demonstrated by RGF, CLE, and TOLS peptides, which all negatively regulate lateral root development in Arabidopsis (*40–42*). It is therefore possible that multiple peptide hormones regulate haustorium development in parasitic plants and each can independently induce prehaustoria in *P. japonicum*. Further work is needed to establish whether additional peptide hormones participate in the *P. japonicum* prehaustorium induction pathway.

Earlier work has shown that *de novo* biosynthesis of auxin through PjYUC3 is essential for haustorium formation (*13*). Consistent with this role, treatment of *P. japonicum* with PjRGF1, PjRGF2, and PjRGF5, like DMBQ, up-regulated *PjYUC3* in root tips (Fig. 1D). This differs from

bioRxiv preprint doi: https://doi.org/10.1101/2025.02.09.637280; this version posted February 10, 2025. The copyright holder for this preprint (which was not certified by peer review) is the author/funder, who has granted bioRxiv a license to display the preprint in perpetuity. It is made available under a CC-BY-NC-ND 4.0 International license.

RGF peptides in Arabidopsis as they are linked to auxin signaling through PIN protein mobilization rather than local auxin biosynthesis (*21*, *22*, *28*). This does not rule out the possibility that PjRGF peptides also influence PjPIN distribution in the haustorium, as there is overlap with the spatial expression pattern of *PjRGF2pro* and *PjRGF5pro* with PjPIN1 and PjPIN2 (Fig. 2B) (*43*). However, PIN inhibition in *P. japonicum* does not impact prehaustorium formation (*43*). Therefore, it is likely that cell-specific up-regulation of *PjYUC3* is the main mechanism through which PjRGFs induce prehaustoria. The RGF peptide pathway in *P. japonicum*, while operating under the distinct context of haustorium formation, likely diverges from Arabidopsis beyond PLT2 stabilization given the fact that PjRGF2 extends the gradient of PjPLT in the RAM in a way reminiscent of RGF peptides in Arabidopsis (Fig. 2C) (*19*, *27*). A similar divergence was observed between CARD1-LIKE-based DMBQ signaling in *P. japonicum* and CARD1-based DMBQ signaling in Arabidopsis (*14*). Therefore, RGF peptide signaling represents another evolutionary innovation in parasitic plants. Further characterization of PjRGF peptides should illuminate additional roles these signals play and the genes they regulate during haustorium development.

The conservation of RGF peptides in plants, coupled with their unique usage in *P. japonicum* and *S. hermonthica* highlights the need to explore how genes evolve in connection with parasitism. Although our current understanding of plant parasitism is limited, the multiplication and neofunctionalization of KAI2d/ShHTL strigolactone receptors from KAI2 in Orobanchaceae serve as a notable precedent (*44*, *45*). Our findings indicate that PjRGF2 and PjRGF5 represent another set of genes co-opted specifically for parasitic function. Phylogenetic analyses revealed that these two peptides acquired haustorial functionality through distinct evolutionary trajectories: PjRGF2 aligns with other Orobanchaceae homologues, while PjRGF5

bioRxiv preprint doi: https://doi.org/10.1101/2025.02.09.637280; this version posted February 10, 2025. The copyright holder for this preprint (which was not certified by peer review) is the author/funder, who has granted bioRxiv a license to display the preprint in perpetuity. It is made available under a CC-BY-NC-ND 4.0 International license.

clusters with non-homologous RGF peptides (Fig. 3B). This implies that PjRGF5 is likely a more recent innovation in *P. japonicum*, arising through a series of tandem duplications and neofunctionalization (Fig. 3A). This may have begun with a duplication of PjRGF8, given the similarity of the PjRGF8 and PjRGF5 prepropeptides and the presence of LTR TEs around *PjRGF8* and *PjRGF5* copies (Fig. 3A,B). Tandem duplication followed by neofunctionalization is not unusual in RGF peptides and is seen in Arabidopsis with RGF7, GLV8, and an uncharacterized RGF peptide AT3g02245 (*46*). PjRGF2, in contrast, is preserved as a single-copy gene in both parasitic and non-parasitic Orobanchaceae species (Fig. 3B,C), suggesting that its parasitism function may have emerged via functional divergence soon after parasitism originated in the family. Investigating the regulatory mechanisms that control *PjRGF2* expression in non-parasitic and parasitic lineages will further unravel the evolution of plant parasitism.

Haustorium development is integral to plant parasitism and RGF signaling is now shown to be essential for prehaustorium formation in *P. japonicum*. Specifically, knockouts of *PjRGFR1* and *PjRGFR3* significantly reduced DMBQ-induced prehaustorium formation (Fig. 5B). In Arabidopsis, two RGFRs similarly regulate lateral root elongation (*20*), reflecting the fact that two RGFRs also govern prehaustorium initiation in *P. japonicum*. Based on our PjRGFR-BRI1 chimera assay, PjRGFR1 is solely activated by PjRGF2, whereas PjRGFR3 is activated by both PjRGF2 and PjRGF5 (Fig 4B,C), implying that PjRGF2 and PjRGF5 act redundantly. As such, a double mutant for *PjRGF2* and *PjRGF5* may be necessary to observe the phenotype seen in *pjrgfr3* and *pjrgfr1* knock-outs. Although ectodomain-BRI1 chimera assays were originally used validate known ligand-receptor pairs (*36*), our results show that they can help pinpoint receptor candidates for endogenous signaling peptides. Thus, although the precise role of PjRGFR4

bioRxiv preprint doi: https://doi.org/10.1101/2025.02.09.637280; this version posted February 10, 2025. The copyright holder for this preprint (which was not certified by peer review) is the author/funder, who has granted bioRxiv a license to display the preprint in perpetuity. It is made available under a CC-BY-NC-ND 4.0 International license.

during haustorium development remains unclear, our results suggest that PjRGFR4 likely responds to both PjRGF2 and PjRGF5 *in planta* (Fig 4B,C). Notably, *PjRGFR4pro* and *PjRGF2pro* expression localize to the base of the haustorium at 1 DPI (Fig. 2B, Fig. 4A), hinting that PjRGFR4 may modulate haustorium development after the initial prehaustorium stage. Therefore, further investigation into the *P. japonicum* RGF signaling pathway could provide enlightenment on haustorium development beyond the initial prehaustorium phase. Collectively, our work establishes endogenous RGF peptides and their cognate receptors as critical components of the haustorium developmental signaling pathway in parasitic plants, paving the way for future studies on how these pathways have evolved and diversified.

Methods

Plant material and growth conditions: *P. japonicum* seeds were surface-sterilized with 50% bleach, sown on ½ MS + 1% sucrose, and stratified at 4°C for one day in the dark. Plates were placed either flat or upright in the growth chamber at 25°C in the dark. After three days, plants were moved to 16-h day / 8-h night cycle (long day (LD) condition). Six-day-old *P. japonicum* seedlings were used for hairy root transformation. Seedlings not used for hairy root transformation were transferred to 0.7% water agar + 4.5 mM MES pH 6.4 after eight days of growth. Eleven-day-old seedlings were then transferred to 2 mL water + 4.5 mM MES pH 6.4 for HIF assays. *A. thaliana* Col-0 seeds were surface-sterilized as previously described, sown on ½ MS + 1% sucrose (*43*), stratified at 4°C for two days, and grown under 22°C LD conditions. Plates were placed upright in the growth chamber for parasitism assays. *N. benthamiana* seeds were surface-sterilized with 50% bleach, sown on ½ MS + 1% sucrose, and placed at 25°C LD

bioRxiv preprint doi: https://doi.org/10.1101/2025.02.09.637280; this version posted February 10, 2025. The copyright holder for this preprint (which was not certified by peer review) is the author/funder, who has granted bioRxiv a license to display the preprint in perpetuity. It is made available under a CC-BY-NC-ND 4.0 International license.

conditions. Seven-day-old *N. benthamiana* seedlings were transferred to 2 mL of water + 4.5 mM MES pH 6.4. *S. hermonthica* seeds were sterilized as previously described and kept in water at 25°C (*8*). After 1 to 2 weeks, seeds were treated with 10 nM strigol to induce germination.

***P. japonicum* hairy root transformation:** Hairy root transformation was performed as previously described with slight modifications (*47*). Briefly, *Agrobacterium rhizogenes* AR1193 strains were streaked from glycerol stocks on LB supplemented with the appropriate antibiotics four days prior to transformation and grown at 28°C. Two days before transformation, streaked *A. rhizogenes* AR1193 was used to seed a 3 mL LB liquid culture that was then grown overnight at 28°C. After 10-14 hours of growth, 1 mL of the *A. rhizogenes* LB culture was added to 5 mL of AB:MES salts and grown overnight at 28°C. The next day the bacteria was pelleted and resuspended in 40 mL of 10 mM $MgCl_2$ + 10 mM MES pH 5.5 + 200 µM acetosyringone + 0.01% Silwet. Six-day old *P. japonicum* seedlings were immersed in this solution as previously described and then transferred to B5 + 1% sucrose + 10 mM MES pH 5.5 + 450 µM acetosyringone agar plates and kept in the dark for two days at 22°C. Seedlings were then transferred to B5 + 1% sucrose + 300 mg/L cefotaxime and kept at 25°C LD conditions. Hairy roots typically emerged in 3 to 4 weeks. Plants with hairy roots were transferred to 0.7% water agar + 0.01% glucose + 100 mg/L Timentin (GoldBio) and were grown for at least four days at 25°C LD conditions before further use.

RT-qPCR and RT-PCR experiments: Twelve-day-old *P. japonicum* that had been equilibrated in water + 4.5 mM MES for one day were treated with DMSO, 10 µM DMBQ, or *N. benthamiana* exudate for six hours. Root tips were collected and flash frozen in liquid nitrogen.

bioRxiv preprint doi: https://doi.org/10.1101/2025.02.09.637280; this version posted February 10, 2025. The copyright holder for this preprint (which was not certified by peer review) is the author/funder, who has granted bioRxiv a license to display the preprint in perpetuity. It is made available under a CC-BY-NC-ND 4.0 International license.

Total RNA was extracted using the Promega max100 RNA isolation machine (Promega). First-strand cDNA was synthesized using ReverTra Ace qPCR RT kit (TOYOBO). RT-qPCR was performed using Thunderbird SYBR qPCR Mix (TOYOBO) on a Stratagene Mx3000p (Agilent). *PjUBC* was used as the internal control (*13*). Primers used in this study can be found in Supplemental Table S6.

For amplifying and sequencing *PjRGF* CDSs, total RNA was separately extracted from *P. japonicum* roots and *P. japonicum* leaves as described above. First-strand cDNA was synthesized as described above. The coding domain sequence (CDS) for *PjRGFs* was amplified from cDNA using KOD ONE (TOYOBO) and run on a 2% agarose gel preloaded with GelGreen (biotium). Bands of the correct size were gel extracted with FastGene Gel/PCR Purification kit (Nippon Genetics) and sent for Sanger sequencing (Eurofins). *PjRGF5* CDSs were subcloned into pENTR/SD/D-TOPO (ThermoFisher) and sent for Sanger sequencing.

Plasmid construction: Promoters (roughly 2.0-2.5 kbp) used for this study were cloned from *P. japonicum* gDNA using KOD ONE, except for *PjRGF5-2b* and *PjRGF5-5*, which were synthesized (Genscript). All promoters were inserted into a binary vector upstream of a 3x-Venus-NLS and Arabidopsis HSP terminator via Infusion (Takara) or HiFi (NEB) assembly. *PjPLT* was cloned from *P. japonicum* gDNA using KOD ONE and *mNeonGreen* (*mNG*) was cloned from pICSL50015 (*48*) using KOD ONE. The *PjPLT* promoter, *mNG*, and *PjPLT* were inserted upstream of an HSP terminator via InFusion assembly. The ecto domain-coding regions for each RGFR were cloned from *P. japonicum* gDNA using KOD ONE and inserted into an ePiGreen vector already containing the coding sequences for *EFR* signal peptide and *BRI1* transmembrane and kinase domains via InFusion (*36*). RUBY was synthesized (Genscript) and

bioRxiv preprint doi: https://doi.org/10.1101/2025.02.09.637280; this version posted February 10, 2025. The copyright holder for this preprint (which was not certified by peer review) is the author/funder, who has granted bioRxiv a license to display the preprint in perpetuity. It is made available under a CC-BY-NC-ND 4.0 International license.

410 then assembled into pGWB4 that was precut with Bsp1407I (ThermoFisher) using InFusion.
411 RUBY was amplified from this vector and transferred to pAGM1310 to make it compatible with
412 golden gate cloning (*49*). zCas9i was originally acquired from pAGM47523 and the bipartite
413 nuclear localization signals were cloned from pFASTRK (*50*, *51*). Primers, plasmids, and strains
414 used in this study can be found in Supplementary Tables S6 and S7.
415
416 ***Agrobacterium* transformation:** *A. rhizogenes* AR1193 and *A. tumafaciens* AGL1 were
417 transformed via electroporation. Following electroporation, cells were recovered in LB medium
418 at 28°C for two hours before being plated in LB agar that contained the appropriate antibiotics
419 and kept at 28°C. Transformed colonies were picked two days after electroporation.
420
421 ***N. benthamiana* transient expression and PjRGFR-BRI1 band shift assay:** *A. tumafaciens*
422 AGL1 strains carrying binary vectors for constitutive expression of *PjRGFR-BRI1-3xHA*, *EFR-*
423 *BRI1-3xHA*, or *BES1-3xHA* were grown overnight in LB media supplemented with the
424 appropriate antibiotics for selection. The following day, the bacteria was pelleted and
425 resuspended in infiltration buffer (10 mM $MgCl_2$, 10 mM MES pH 5.5, 200 µM acetosyringone).
426 The bacterial concentration was then adjusted to an OD600 of 0.5 for the LRR-BRI1-3xHA
427 constructs and 0.25 for the BES1-3xHA constructs before being co-infiltrated into *N.*
428 *benthamiana* leaves. 100 nM of PjRGF2 or PjRGF5 were infiltrated three days post *A.*
429 *tumafaciens* infiltration. Three four mm leaf discs were collected at 0 and 30 minutes after
430 PjRGF2/5 infiltration. Western blots were performed as described in Ngou et al. (*36*).
431

bioRxiv preprint doi: https://doi.org/10.1101/2025.02.09.637280; this version posted February 10, 2025. The copyright holder for this preprint (which was not certified by peer review) is the author/funder, who has granted bioRxiv a license to display the preprint in perpetuity. It is made available under a CC-BY-NC-ND 4.0 International license.

Confocal microscopy: *P. japonicum* hairy roots were placed on glass bottom dishes, covered with 0.7% water agar, and allowed to acclimate for one day at 25°C LD conditions. Transformed hairy roots were then observed on a Leica SP8 WLL FALCON confocal microscope with a white light laser (WLL). Roots were treated with 10 µM DMBQ, 10 nM PjRGF2, or placed next to a host root and observed one day and two days after treatment. Additionally, *P. japonicum* roots fixed with 4% paraformaldehyde and cleared for four days in ClearSeeAlpha were stained with calcofluor white and basic fuschin (*52*, *53*). These roots were mounted on SlowFade Diamond antifade mountant (ThermoFisher) and observed on a Leica SP8 WLL FALCON confocal microscope using 405 nm diode laser and WLL illumination.

Nitro blue tetrazolium staining: *P. japonicum* seedlings were treated with either 10 µM DMBQ or DMSO. Seedlings were then taken at one- or two-days post treatment and stained with a 0.1% nitro blue tetrazolium salt (NBT; Fujifilm Wako) solution for 30-40 minutes in the dark. Roots that had a prehaustorium were excised and mounted on a slide. NBT staining was observed on an Olympus BX52 microscope (Olympus).

***P. japonicum* genome sequencing:** Genomic DNA was extracted using hexadecyltrimethylammonium bromide (CTAB) method (*30*). Healthy leaves from about one-month-old *P. japonicum* (ecotype Okayama) were flash frozen under liquid nitrogen, ground, and added into 3× volume of 2×CTAB buffer [consisting of 2% CTAB, 100 mM Tris-HCl (pH 8.0), 20 mM ethylenediaminetetraacetic acid (EDTA), 1.4 M NaCl, 2% polyvinylpyrrolidone (PVP) and 0.1% β-mercaptoethanol] on a stirring hot plate. The solution was transferred to 50 mL falcon tube and shaken at 60ºC for 40 minutes before adding 1× volume of chloroform and

bioRxiv preprint doi: https://doi.org/10.1101/2025.02.09.637280; this version posted February 10, 2025. The copyright holder for this preprint (which was not certified by peer review) is the author/funder, who has granted bioRxiv a license to display the preprint in perpetuity. It is made available under a CC-BY-NC-ND 4.0 International license.

gently mixed in a rotator at room temperature for 10 min. After centrifuging at 3500 rpm for 20 min at room temperature, aqueous phase was transferred to a new tube, 0.1× volume of 10% CTAB (consisting of 10% CTAB and 0.7 M NaCl) and 1× volume of chloroform was added. The solution was rotated gently for 10 min before being centrifuged at 3,500 rpm for 20 min. The aqueous phase was transferred to a new tube, 1× volume of isopropanol was then added and mixed gently. The solution was centrifuged at 10,000 rpm for 30 min, supernatant was discarded, and the pellet was washed with 70% ethanol. Centrifugation at 10000 rpm was repeated for 10 min. Supernatant was discarded, pellet was dissolved in 500 µL TE solution and followed by QIAGEN Genomic-tip 100/G following manufacturer's instructions. Long read sequencing libraries were prepared using the SMRTbell Express Template Prep Kit (PacBio). Sequencing was performed on a PacBio Sequel. Long read sequences (x 48 coverage) were assembled using canu (ver1.8) with default setting (*54*). Genes were annotated using Exonerate (ver2.2) and transposable elements were predicted using HiTE (ver3.2.0) (*55*, *56*).

Alignments and phylogeny: Sequences for studied peptides and proteins were aligned using MUSCLE (ver3.8.1551) (*57*). Alignments were rendered with ESPRIT 3.0 (*58*). The maximum-likelihood phylogenetic tree for RGF prepropeptides was constructed using MEGA11 with a bootstrap value of 100, while for AP2 transcription factors phylogenetic tree Ugene (ver48.1) was used with a bootstrap value of 100 (*59*, *60*). RGFR sequences from 355 species were taken from Ngou et al (*61*). The RGFRs from five additional Orobanchaceae species were added to this group to make a group of RGFRs from 360 species. Sequences were aligned and phylogenetic trees were constructed as described by Ngou et al (*61*). EFR and its homologues were used as an outgroup.

bioRxiv preprint doi: https://doi.org/10.1101/2025.02.09.637280; this version posted February 10, 2025. The copyright holder for this preprint (which was not certified by peer review) is the author/funder, who has granted bioRxiv a license to display the preprint in perpetuity. It is made available under a CC-BY-NC-ND 4.0 International license.

Identification of unannotated RGF peptides in *P. japonicum* genome: Unannotated RGF peptides in *P. japonicum* were identified through tBLASTn using a list of the mature sequence of RGF peptides from 21 species as well as reciprocal tBLASTn of the mature sequence of PjRGFs. The 5' and 3' ends of the CDS for the RGF prepropeptide were mapped using RNA-seq data and then the sequence for the prepropeptide was amplified from *P. japonicum* cDNA. Amplified sequences were sent for sequencing. Unannotated RGF peptides from *P. cranolopha*, *P. kansuensis*, *L. lindenbergia*, and *L. phillipensis* were identified as described above. A putative prepropeptide CDS was determined using the homologous *P. japonicum* prepropeptide as a guide.

***P. japonicum* and *S. hermonthica* HIF assays:** Twelve-day-old *P. japonicum* seedling or hairy roots, equilibrated in ddH_2O + 4.5 mM MES pH 6.4 + 100 µM Timentin (for hairy roots) + 0.01% glucose (for hairy roots) were treated with 10 µM DMBQ or synthesized PjRGF peptides (Peptide Institute and Genscript) at varying concentrations or DMSO. Haustorium formation was scored two days after treatment. One-day-old *S. hermonthica* was treated with 10 µM DMBQ, 5 nM synthesized ShRGF peptides, DMSO, or H_2O. Haustorium formation was scored at one and two days after treatment.

Guide RNA design: Guide RNAs were designed using CHOPCHOP, selected for high predicted efficiency and specificity to each target gene (*62*).

bioRxiv preprint doi: https://doi.org/10.1101/2025.02.09.637280; this version posted February 10, 2025. The copyright holder for this preprint (which was not certified by peer review) is the author/funder, who has granted bioRxiv a license to display the preprint in perpetuity. It is made available under a CC-BY-NC-ND 4.0 International license.

CRISPR hairy root sequencing: Hairy roots from *P. japonicum* expressing gRNAs and zCAS9i were individually frozen and then macerated. Genomic DNA (gDNA) extraction buffer (200 mM Tris-HCl pH 7.5, 250 mM NaCl, 25 mM EDTA, 0.5% (w/v) SDS) was added, followed by 99% ethanol (2:1 ratio) to precipitate the gDNA, which was then resuspended in TE pH 8.0. The target region along with a small flanking region on either side was amplified from the extracted gDNA and subcloned into pUC19. Three subcloned colonies were sequenced to verify editing events.

Statistical analysis: Statistical analysis was performed on R (ver4.3.2).

RNA-seq analysis: *P. japonicum* seedlings were germinated and grown in 1/2 MS liquid medium supplemented with 0.25% sucrose under long-day conditions at 25 °C. After 2 weeks 5 µM DMBQ and DMSO as a mock control were supplemented to the liquid media, then whole seedlings were collected and snap-frozen at six time points: 0 h, 10 min, 30 min, 1 h, 6 h, and 24 h. Total RNA was extracted using RNeasy Plant mini kit (Qiagen). RNA-seq libraries were prepared with the KAPA mRNA HyperPrep Kit (Roche) according to the manufacturer's directions. NEBNext Multiplex Oligos for Illumina (NEB) was used for the adaptor ligation step. Sequencing was performed on a NextSeq500 platform (single-end, 75 bp). Reads were quality controlled using fastp (ver0.24.0) (*63*), then mapped to the *P. japonicum* genome (*30*) using STAR aligner (ver2.7.11) (*64*). Read counts per gene were obtained using featureCounts in Subread (ver2.0.8) (*65*). Differentially expressed genes (DEGs) in DMBQ treatment samples were calculated using edgeR (ver4.0.16) with glmQLFTest function (*66*), following filtering out low expression genes using filterByExpr function with the default parameters and subsequent

bioRxiv preprint doi: https://doi.org/10.1101/2025.02.09.637280; this version posted February 10, 2025. The copyright holder for this preprint (which was not certified by peer review) is the author/funder, who has granted bioRxiv a license to display the preprint in perpetuity. It is made available under a CC-BY-NC-ND 4.0 International license.

523 trimmed mean of M-values normalization. DEG detection result was provided in Supplemental
524 table S1.
525
526 References
527
528 1. J. H. Westwood, J. I. Yoder, M. P. Timko, C. W. dePamphilis, The evolution of parasitism in
529 plants. *Trends Plant Sci.* **15**, 227–235 (2010).

530 2. S. Yoshida, S. Cui, Y. Ichihashi, K. Shirasu, The haustorium, a specialized invasive organ in
531 parasitic plants. *Annu. Rev. Plant Biol.* **67**, 643–667 (2016).

532 3. C. R. Clarke, M. P. Timko, J. I. Yoder, M. J. Axtell, J. H. Westwood, Molecular Dialog
533 Between Parasitic Plants and Their Hosts. *Annu. Rev. Phytopathol.* **57**, 279–299 (2019).

534 4. J. M. Mutuku, S. Cui, S. Yoshida, K. Shirasu, Orobanchaceae parasite–host interactions. *New*
535 *Phytol.* **230**, 46–59 (2021).

536 5. D. Cartry, C. Steinberg, S. Gibot-Leclerc, Main drivers of broomrape regulation. A review.
537 *Agron. Sustain. Dev.* **41**, 17 (2021).

538 6. Y. Xu, J. Zhang, C. Ma, Y. Lei, G. Shen, J. Jin, D. A. R. Eaton, J. Wu, Comparative genomics
539 of orobanchaceous species with different parasitic lifestyles reveals the origin and stepwise
540 evolution of plant parasitism. *Mol. Plant* **15**, 1384–1399 (2022).

541 7. T. Wakatake, S. Yoshida, K. Shirasu, Induced cell fate transitions at multiple cell layers
542 configure haustorium development in parasitic plants. *Development* **145**, dev164848
543 (2018).

bioRxiv preprint doi: https://doi.org/10.1101/2025.02.09.637280; this version posted February 10, 2025. The copyright holder for this preprint (which was not certified by peer review) is the author/funder, who has granted bioRxiv a license to display the preprint in perpetuity. It is made available under a CC-BY-NC-ND 4.0 International license.

8. S. Cui, S. Wada, Y. Tobimatsu, Y. Takeda, S. B. Saucet, T. Takano, T. Umezawa, K. Shirasu, S. Yoshida, Host lignin composition affects haustorium induction in the parasitic plants Phtheirospermum japonicum and Striga hermonthica. *New Phytol.* **218**, 710–723 (2018).

9. M. Chang, D. G. Lynn, The haustorium and the chemistry of host recognition in parasitic angiosperms. *J. Chem. Ecol.* **12**, 561–579 (1986).

10. V. Goyet, S. Wada, S. Cui, T. Wakatake, K. Shirasu, G. Montiel, P. Simier, S. Yoshida, Haustorium Inducing Factors for Parasitic Orobanchaceae. *Front. Plant Sci.* **10** (2019).

11. V. Goyet, E. Billard, J.-B. Pouvreau, M.-M. Lechat, S. Pelletier, M. Bahut, F. Monteau, L. Spíchal, P. Delavault, G. Montiel, P. Simier, Haustorium initiation in the obligate parasitic plant Phelipanche ramosa involves a host-exudated cytokinin signal. *J. Exp. Bot.* **68**, 5539–5552 (2017).

12. M. Fernández-Aparicio, M. Masi, L. Maddau, A. Cimmino, M. Evidente, D. Rubiales, A. Evidente, Induction of Haustorium Development by Sphaeropsidones in Radicles of the Parasitic Weeds Striga and Orobanche. A Structure–Activity Relationship Study. *J. Agric. Food Chem.* **64**, 5188–5196 (2016).

13. J. K. Ishida, T. Wakatake, S. Yoshida, Y. Takebayashi, H. Kasahara, E. Wafula, C. W. dePamphilis, S. Namba, K. Shirasu, Local Auxin Biosynthesis Mediated by a YUCCA Flavin Monooxygenase Regulates Haustorium Development in the Parasitic Plant Phtheirospermum japonicum. *Plant Cell* **28**, 1795–1814 (2016).

bioRxiv preprint doi: https://doi.org/10.1101/2025.02.09.637280; this version posted February 10, 2025. The copyright holder for this preprint (which was not certified by peer review) is the author/funder, who has granted bioRxiv a license to display the preprint in perpetuity. It is made available under a CC-BY-NC-ND 4.0 International license.

14. A. Laohavisit, T. Wakatake, N. Ishihama, H. Mulvey, K. Takizawa, T. Suzuki, K. Shirasu, Quinone perception in plants via leucine-rich-repeat receptor-like kinases. *Nature* **587**, 92–97 (2020).

15. N. Aoki, S. Cui, S. Yoshida, Cytokinins Induce Prehaustoria Coordinately with Quinone Signals in the Parasitic Plant Striga hermonthica. *Plant Cell Physiol.* **63**, 1446–1456 (2022).

16. P. C. G. Bandaranayake, T. Filappova, A. Tomilov, N. B. Tomilova, D. Jamison-McClung, Q. Ngo, K. Inoue, J. I. Yoder, A Single-Electron Reducing Quinone Oxidoreductase Is Necessary to Induce Haustorium Development in the Root Parasitic Plant Triphysaria. *Plant Cell* **22**, 1404–1419 (2010).

17. P. C. G. Bandaranayake, A. Tomilov, N. B. Tomilova, Q. A. Ngo, N. Wickett, C. W. dePamphilis, J. I. Yoder, The TvPirin Gene Is Necessary for Haustorium Development in the Parasitic Plant Triphysaria versicolor. *Plant Physiol.* **158**, 1046–1053 (2012).

18. S. Wada, S. Cui, S. Yoshida, Reactive Oxygen Species (ROS) Generation Is Indispensable for Haustorium Formation of the Root Parasitic Plant Striga hermonthica. *Front. Plant Sci.* **10**, 328 (2019).

19. Y. Matsuzaki, M. Ogawa-Ohnishi, A. Mori, Y. Matsubayashi, Secreted Peptide Signals Required for Maintenance of Root Stem Cell Niche in Arabidopsis. *Science* **329**, 1065–1067 (2010).

20. A. I. Fernandez, N. Vangheluwe, K. Xu, J. Jourquin, L. A. N. Claus, S. Morales-Herrera, B. Parizot, H. De Gernier, Q. Yu, A. Drozdzecki, T. Maruta, K. Hoogewijs, W. Vannecke, B. Peterson, D. Opdenacker, A. Madder, Z. L. Nimchuk, E. Russinova, T. Beeckman,

bioRxiv preprint doi: https://doi.org/10.1101/2025.02.09.637280; this version posted February 10, 2025. The copyright holder for this preprint (which was not certified by peer review) is the author/funder, who has granted bioRxiv a license to display the preprint in perpetuity. It is made available under a CC-BY-NC-ND 4.0 International license.

584 GOLVEN peptide signalling through RGI receptors and MPK6 restricts asymmetric cell
585 division during lateral root initiation. *Nat. Plants* **6**, 533–543 (2020).

586 21. K. Xu, J. Jourquin, X. Xu, I. De Smet, A. I. Fernandez, T. Beeckman, Dynamic GOLVEN-
587 ROOT GROWTH FACTOR 1 INSENSITIVE signaling in the root cap mediates root
588 gravitropism. *Plant Physiol.* **192**, 256–273 (2023).

589 22. J. Jourquin, A. I. Fernandez, Q. Wang, K. Xu, J. Chen, J. Šimura, K. Ljung, S. Vanneste, T.
590 Beeckman, GOLVEN peptides regulate lateral root spacing as part of a negative feedback
591 loop on the establishment of auxin maxima. *J. Exp. Bot.* **74**, 4031–4049 (2023).

592 23. C. Furumizu, S. Sawa, The RGF/GLV/CLEL Family of Short Peptides Evolved Through
593 Lineage-Specific Losses and Diversification and Yet Conserves Its Signaling Role Between
594 Vascular Plants and Bryophytes. *Front. Plant Sci.* **12** (2021).

595 24. W. Song, L. Liu, J. Wang, Z. Wu, H. Zhang, J. Tang, G. Lin, Y. Wang, X. Wen, W. Li, Z.
596 Han, H. Guo, J. Chai, Signature motif-guided identification of receptors for peptide
597 hormones essential for root meristem growth. *Cell Res.* **26**, 674–685 (2016).

598 25. Y. Ou, X. Lu, Q. Zi, Q. Xun, J. Zhang, Y. Wu, H. Shi, Z. Wei, B. Zhao, X. Zhang, K. He, X.
599 Gou, C. Li, J. Li, RGF1 INSENSITIVE 1 to 5, a group of LRR receptor-like kinases, are
600 essential for the perception of root meristem growth factor 1 in Arabidopsis thaliana. *Cell*
601 *Res.* **26**, 686–698 (2016).

602 26. H. Shinohara, A. Mori, N. Yasue, K. Sumida, Y. Matsubayashi, Identification of three LRR-
603 RKs involved in perception of root meristem growth factor in Arabidopsis. *Proc. Natl.*
604 *Acad. Sci. U. S. A.* **113**, 3897–3902 (2016).

bioRxiv preprint doi: https://doi.org/10.1101/2025.02.09.637280; this version posted February 10, 2025. The copyright holder for this preprint (which was not certified by peer review) is the author/funder, who has granted bioRxiv a license to display the preprint in perpetuity. It is made available under a CC-BY-NC-ND 4.0 International license.

605 27. M. Yamada, X. Han, P. N. Benfey, RGF1 controls root meristem size through ROS
606 signalling. *Nature* **577**, 85–88 (2020).

607 28. R. Whitford, A. Fernandez, R. Tejos, A. C. Pérez, J. Kleine-Vehn, S. Vanneste, A.
608 Drozdzecki, J. Leitner, L. Abas, M. Aerts, K. Hoogewijs, P. Baster, R. De Groodt, Y.-C. Lin,
609 V. Storme, Y. Van de Peer, T. Beeckman, A. Madder, B. Devreese, C. Luschnig, J. Friml, P.
610 Hilson, GOLVEN Secretory Peptides Regulate Auxin Carrier Turnover during Plant
611 Gravitropic Responses. *Dev. Cell* **22**, 678–685 (2012).

612 29. S. Ogawa, T. Wakatake, T. Spallek, J. K. Ishida, R. Sano, T. Kurata, T. Demura, S. Yoshida,
613 Y. Ichihashi, A. Schaller, K. Shirasu, Subtilase activity in intrusive cells mediates
614 haustorium maturation in parasitic plants. *Plant Physiol.* **185**, 1381–1394 (2021).

615 30. S. Cui, T. Kubota, T. Nishiyama, J. K. Ishida, S. Shigenobu, T. F. Shibata, A. Toyoda, M.
616 Hasebe, K. Shirasu, S. Yoshida, Ethylene signaling mediates host invasion by parasitic
617 plants. *Sci. Adv.* **6**, eabc2385 (2020).

618 31. A. Fernandez, A. Drozdzecki, K. Hoogewijs, A. Nguyen, T. Beeckman, A. Madder, P. Hilson,
619 Transcriptional and Functional Classification of the GOLVEN/ROOT GROWTH
620 FACTOR/CLE-Like Signaling Peptides Reveals Their Role in Lateral Root and Hair
621 Formation. *Plant Physiol.* **161**, 954–970 (2013).

622 32. S. Qiu, J. M. Bradley, P. Zhang, R. Chaudhuri, M. Blaxter, R. K. Butlin, J. D. Scholes,
623 Genome-enabled discovery of candidate virulence loci in Striga hermonthica, a devastating
624 parasite of African cereal crops. *New Phytol.* **236**, 622–638 (2022).

bioRxiv preprint doi: https://doi.org/10.1101/2025.02.09.637280; this version posted February 10, 2025. The copyright holder for this preprint (which was not certified by peer review) is the author/funder, who has granted bioRxiv a license to display the preprint in perpetuity. It is made available under a CC-BY-NC-ND 4.0 International license.

33. S. Yoshida, S. Kim, E. K. Wafula, J. Tanskanen, Y.-M. Kim, L. Honaas, Z. Yang, T. Spallek, C. E. Conn, Y. Ichihashi, K. Cheong, S. Cui, J. P. Der, H. Gundlach, Y. Jiao, C. Hori, J. K. Ishida, H. Kasahara, T. Kiba, M.-S. Kim, N. Koo, A. Laohavisit, Y.-H. Lee, S. Lumba, P. McCourt, J. C. Mortimer, J. M. Mutuku, T. Nomura, Y. Sasaki-Sekimoto, Y. Seto, Y. Wang, T. Wakatake, H. Sakakibara, T. Demura, S. Yamaguchi, K. Yoneyama, R. Manabe, D. C. Nelson, A. H. Schulman, M. P. Timko, C. W. dePamphilis, D. Choi, K. Shirasu, Genome Sequence of *Striga asiatica* Provides Insight into the Evolution of Plant Parasitism. *Curr. Biol.* **29**, 3041-3052.e4 (2019).

34. L. Fang, M. Li, J. Zhang, C. Jia, Y. Qiang, X. He, T. Liu, Q. Zhou, D. Luo, Y. Han, Z. Li, W. Liu, Y. Yang, J. Liu, Z. Liu, Chromosome-level genome assembly of Pedicularis kansuensis illuminates genome evolution of facultative parasitic plant. *Mol. Ecol. Resour.* **24**, e13966 (2024).

35. D. M. Goodstein, S. Shu, R. Howson, R. Neupane, R. D. Hayes, J. Fazo, T. Mitros, W. Dirks, U. Hellsten, N. Putnam, D. S. Rokhsar, Phytozome: a comparative platform for green plant genomics. *Nucleic Acids Res.* **40**, D1178–D1186 (2012).

36. B. P. M. Ngou, M. Wyler, M. W. Schmid, Y. Kadota, K. Shirasu, Evolutionary trajectory of pattern recognition receptors in plants. *Nat. Commun.* **15**, 308 (2024).

37. A. Greifenhagen, I. Braunstein, J. Pfannstiel, S. Yoshida, K. Shirasu, A. Schaller, T. Spallek, The Phtheirospermum japonicum isopentenyltransferase PjIPT1a regulates host cytokinin responses in Arabidopsis. *New Phytol.* **232**, 1582–1590 (2021).

bioRxiv preprint doi: https://doi.org/10.1101/2025.02.09.637280; this version posted February 10, 2025. The copyright holder for this preprint (which was not certified by peer review) is the author/funder, who has granted bioRxiv a license to display the preprint in perpetuity. It is made available under a CC-BY-NC-ND 4.0 International license.

38. R. Grützner, P. Martin, C. Horn, S. Mortensen, E. J. Cram, C. W. T. Lee-Parsons, J. Stuttmann, S. Marillonnet, High-efficiency genome editing in plants mediated by a Cas9 gene containing multiple introns. *Plant Commun.* **2** (2021).

39. A. Greifenhagen, H. Ruwe, V. Zimmer, J. Messerschmidt, D. P. N. Bhukya, H. D. Kenea, A. Schaller, T. Spallek, The peptide hormone PjCLE1 stimulates haustorium formation in the parasitic plant Phtheirospermum japonicum. *Proc. Natl. Acad. Sci.* **121**, e2414582121 (2024).

40. J. Jourquin, A. I. Fernandez, B. Parizot, K. Xu, W. Grunewald, A. Mamiya, H. Fukaki, T. Beeckman, Two phylogenetically unrelated peptide-receptor modules jointly regulate lateral root initiation via a partially shared signaling pathway in Arabidopsis thaliana. *New Phytol.* **233**, 1780–1796 (2022).

41. S. Nakagami, T. Aoyama, Y. Sato, T. Kajiwara, T. Ishida, S. Sawa, CLE3 and its homologs share overlapping functions in the modulation of lateral root formation through CLV1 and BAM1 in Arabidopsis thaliana. *Plant J.* **113**, 1176–1191 (2023).

42. K. Toyokura, T. Goh, H. Shinohara, A. Shinoda, Y. Kondo, Y. Okamoto, T. Uehara, K. Fujimoto, Y. Okushima, Y. Ikeyama, K. Nakajima, T. Mimura, M. Tasaka, Y. Matsubayashi, H. Fukaki, Lateral Inhibition by a Peptide Hormone-Receptor Cascade during *Arabidopsis* Lateral Root Founder Cell Formation. *Dev. Cell* **48**, 64-75.e5 (2019).

43. T. Wakatake, S. Ogawa, S. Yoshida, K. Shirasu, An auxin transport network underlies xylem bridge formation between the hemi-parasitic plant Phtheirospermum japonicum and host Arabidopsis. *Development* **147**, dev187781 (2020).

bioRxiv preprint doi: https://doi.org/10.1101/2025.02.09.637280; this version posted February 10, 2025. The copyright holder for this preprint (which was not certified by peer review) is the author/funder, who has granted bioRxiv a license to display the preprint in perpetuity. It is made available under a CC-BY-NC-ND 4.0 International license.

666 44. S. Toh, D. Holbrook-Smith, P. J. Stogios, O. Onopriyenko, S. Lumba, Y. Tsuchiya, A.
667 Savchenko, P. McCourt, Structure-function analysis identifies highly sensitive strigolactone
668 receptors in Striga. *Science* **350**, 203–207 (2015).

669 45. C. E. Conn, R. Bythell-Douglas, D. Neumann, S. Yoshida, B. Whittington, J. H. Westwood,
670 K. Shirasu, C. S. Bond, K. A. Dyer, D. C. Nelson, Convergent evolution of strigolactone
671 perception enabled host detection in parasitic plants. *Science* **349**, 540–543 (2015).

672 46. A. H. Hastwell, X. Chu, Y. Liu, B. J. Ferguson, The parallel narrative of RGF/GLV/CLEL
673 peptide signalling. *Trends Plant Sci.* **29**, 1342–1355 (2024).

674 47. J. K. Ishida, S. Yoshida, M. Ito, S. Namba, K. Shirasu, Agrobacterium rhizogenes-Mediated
675 Transformation of the Parasitic Plant Phtheirospermum japonicum. *PLOS ONE* **6**, e25802
676 (2011).

677 48. C. Engler, M. Youles, R. Gruetzner, T.-M. Ehnert, S. Werner, J. D. G. Jones, N. J. Patron, S.
678 Marillonnet, A Golden Gate Modular Cloning Toolbox for Plants. *ACS Synth. Biol.* **3**, 839–
679 843 (2014).

680 49. C. Engler, M. Youles, R. Gruetzner, T.-M. Ehnert, S. Werner, J. D. G. Jones, N. J. Patron, S.
681 Marillonnet, A Golden Gate Modular Cloning Toolbox for Plants. *ACS Synth. Biol.* **3**, 839–
682 843 (2014).

683 50. R. Grützner, P. Martin, C. Horn, S. Mortensen, E. J. Cram, C. W. T. Lee-Parsons, J.
684 Stuttmann, S. Marillonnet, High-efficiency genome editing in plants mediated by a Cas9
685 gene containing multiple introns. *Plant Commun.* **2**, 100135 (2021).

bioRxiv preprint doi: https://doi.org/10.1101/2025.02.09.637280; this version posted February 10, 2025. The copyright holder for this preprint (which was not certified by peer review) is the author/funder, who has granted bioRxiv a license to display the preprint in perpetuity. It is made available under a CC-BY-NC-ND 4.0 International license.

686 51. W. Develtere, W. Decaestecker, D. Rombaut, C. Anders, E. Clicque, M. Vuylsteke, T. B.
687 Jacobs, Continual improvement of CRISPR-induced multiplex mutagenesis in Arabidopsis.
688 *Plant J.* **119**, 1158–1172 (2024).

689 52. D. Kurihara, Y. Mizuta, S. Nagahara, T. Higashiyama, ClearSeeAlpha: Advanced Optical
690 Clearing for Whole-Plant Imaging. *Plant Cell Physiol.* **62**, 1302–1310 (2021).

691 53. R. Ursache, T. G. Andersen, P. Marhavý, N. Geldner, A protocol for combining fluorescent
692 proteins with histological stains for diverse cell wall components. *Plant J.* **93**, 399–412
693 (2018).

694 54. S. Koren, B. P. Walenz, K. Berlin, J. R. Miller, N. H. Bergman, A. M. Phillippy, Canu:
695 scalable and accurate long-read assembly via adaptive k-mer weighting and repeat
696 separation. *Genome Res.* **27**, 722–736 (2017).

697 55. G. S. C. Slater, E. Birney, Automated generation of heuristics for biological sequence
698 comparison. *BMC Bioinformatics* **6**, 31 (2005).

699 56. K. Hu, P. Ni, M. Xu, Y. Zou, J. Chang, X. Gao, Y. Li, J. Ruan, B. Hu, J. Wang, HiTE: a fast
700 and accurate dynamic boundary adjustment approach for full-length transposable element
701 detection and annotation. *Nat. Commun.* **15**, 5573 (2024).

702 57. R. C. Edgar, Muscle5: High-accuracy alignment ensembles enable unbiased assessments of
703 sequence homology and phylogeny. *Nat. Commun.* **13**, 6968 (2022).

704 58. X. Robert, P. Gouet, Deciphering key features in protein structures with the new ENDscript
705 server. *Nucleic Acids Res.* **42**, W320–W324 (2014).

bioRxiv preprint doi: https://doi.org/10.1101/2025.02.09.637280; this version posted February 10, 2025. The copyright holder for this preprint (which was not certified by peer review) is the author/funder, who has granted bioRxiv a license to display the preprint in perpetuity. It is made available under a CC-BY-NC-ND 4.0 International license.

59. K. Tamura, G. Stecher, S. Kumar, MEGA11: Molecular Evolutionary Genetics Analysis Version 11. *Mol. Biol. Evol.* **38**, 3022–3027 (2021).

60. K. Okonechnikov, O. Golosova, M. Fursov, the UGENE team, Unipro UGENE: a unified bioinformatics toolkit. *Bioinformatics* **28**, 1166–1167 (2012).

61. B. P. M. Ngou, R. Heal, M. Wyler, M. W. Schmid, J. D. G. Jones, Concerted expansion and contraction of immune receptor gene repertoires in plant genomes. *Nat. Plants* **8**, 1146–1152 (2022).

62. K. Labun, T. G. Montague, M. Krause, Y. N. Torres Cleuren, H. Tjeldnes, E. Valen, CHOPCHOP v3: expanding the CRISPR web toolbox beyond genome editing. *Nucleic Acids Res.* **47**, W171–W174 (2019).

63. S. Chen, Ultrafast one-pass FASTQ data preprocessing, quality control, and deduplication using fastp. *iMeta* **2**, e107 (2023).

64. A. Dobin, C. A. Davis, F. Schlesinger, J. Drenkow, C. Zaleski, S. Jha, P. Batut, M. Chaisson, T. R. Gingeras, STAR: ultrafast universal RNA-seq aligner. *Bioinformatics* **29**, 15–21 (2013).

65. Y. Liao, G. K. Smyth, W. Shi, featureCounts: an efficient general purpose program for assigning sequence reads to genomic features. *Bioinformatics* **30**, 923–930 (2014).

66. M. D. Robinson, D. J. McCarthy, G. K. Smyth, edgeR: a Bioconductor package for differential expression analysis of digital gene expression data. *Bioinformatics* **26**, 139–140 (2010).

bioRxiv preprint doi: https://doi.org/10.1101/2025.02.09.637280; this version posted February 10, 2025. The copyright holder for this preprint (which was not certified by peer review) is the author/funder, who has granted bioRxiv a license to display the preprint in perpetuity. It is made available under a CC-BY-NC-ND 4.0 International license.

67. M. Fernández-Aparicio, K. Huang, E. K. Wafula, L. A. Honaas, N. J. Wickett, M. P. Timko, C. W. dePamphilis, J. I. Yoder, J. H. Westwood, Application of qRT-PCR and RNA-Seq analysis for the identification of housekeeping genes useful for normalization of gene expression values during Striga hermonthica development. *Mol. Biol. Rep.* **40**, 3395–3407 (2013).

68. M. G. Heisler, C. Ohno, P. Das, P. Sieber, G. V. Reddy, J. A. Long, E. M. Meyerowitz, Patterns of Auxin Transport and Gene Expression during Primordium Development Revealed by Live Imaging of the *Arabidopsis* Inflorescence Meristem. *Curr. Biol.* **15**, 1899–1911 (2005).

Acknowledgements: We would like to thank Ms. Yoko Nagai for her technical support. The authors would also like to thank Bruno Ngou and Yasu Kadota for their helpful conversations and suggestions in regard to the PjRGFR-BRI1 chimera assays and for Bruno's help in compiling the RGFRs from 355 species. Computations were partially performed on the NIG supercomputer at ROIS National Institute of Genetics.

Funding: M.F. and A.G. are funded by Japan Society for the Promotion of Science Postdoctoral Research Fellowships. This work was supported by JSPS (JP19F19782, JP22H00364, JP20H05909, JP24KF0094), JST (JPMJGX23B2/GteX, JPMJAP2306/ASPIRE), and RIKEN TRIP initiative (to K.S.). This work was also partially supported by JSPS (JP21H02506), JST PRESTO (JPMJPR194D) and Mitsubishi Foundation (to S.Y.).

bioRxiv preprint doi: https://doi.org/10.1101/2025.02.09.637280; this version posted February 10, 2025. The copyright holder for this preprint (which was not certified by peer review) is the author/funder, who has granted bioRxiv a license to display the preprint in perpetuity. It is made available under a CC-BY-NC-ND 4.0 International license.

748

749 **Author contributions:** M.R.F. and K.S conceptualized the study; methodology, M.F., A.G.,
750 T.W., A.L., S.M., A.S., and S.Y.; data acquisition, M.R.F, A.G., T.W., A.L., R.H., S.M., A.S., and
751 S.Y.; formal analysis, M.F., A.G., T.W., and S.Y.; Data curation, M.F., A.G., T.W., and S.Y.;
752 writing, M.F., A.G., T.W., S.Y., and K.S.; Supervision, K.S.; project administration, K.S.; funding
753 acquisition, K.S., S.Y., M.F., and A.G.

754

755 **Competing interests:** The authors declare they have no competing interests. All data needed to
756 evaluate the conclusions in the paper are present in the paper and/or the Supplementary
757 Materials.

758

759 **Figure Legends**

760

761 **Fig. 1. PjRGF peptides induce prehaustoria.** A) Multiple sequence alignment of the C-
762 terminus of the identified RGF peptides in *P. japonicum* and eight of the eleven RGF peptides in
763 Arabidopsis. B) Change in expression of the identified PjRGF peptides six hours post 10 µM
764 DMBQ treatment or *N. benthamiana* treatment as compared to treatment with DMSO. Each dot
765 represents the fold-change per biological replicate. *PjRGF5* was consistently up-regulated
766 however the high-variability between replicates caused the p-value to be > 0.1. Student's T-test
767 was used to determine statistical significance. * represents p-value < 0.05 **represents p-value <
768 0.1. C) Percent of *P. japonicum* forming at least one prehaustorium two day post treatment with
769 DMBQ, PjRGF1, PjRGF2, or PjRGF5. One-way ANOVA followed by Tukey HSD was used for
770 identifying statistical significance. D) Confocal images of *P. japonicum* two days after treatment

bioRxiv preprint doi: https://doi.org/10.1101/2025.02.09.637280; this version posted February 10, 2025. The copyright holder for this preprint (which was not certified by peer review) is the author/funder, who has granted bioRxiv a license to display the preprint in perpetuity. It is made available under a CC-BY-NC-ND 4.0 International license.

771 with 10 µM DMBQ, 2 µM PjRGF1, 5 nM PjRGF2, or 2 µM PjRGF5 stained with calcofluor
772 white (white) and basic fuschin (red). Scale bars = 75 µm. E) Change in expression of *PjYUC3*
773 six hours post treatment with 10 µM DMBQ, 2 µM PjRGF1, 5 nM PjRGF2, or 2 µM PjRGF5.
774
775 **Fig. 2. Hausotrial expression dynamics of *PjRGF* peptides and downstream signaling**
776 **events.** A) Expression of *3x-Venus-NLS* driven by the *DR5* promoter following 1 day post
777 treatment (DPT) 10 µM DMBQ, 2 DPT 5 nM PjRGF2, and at 1 one day post infection (DPI).
778 *DR5* expression, which correlates with auxin localization, occurs at the epidermal cells at the
779 apex of the prehaustorium in all treatments. B) Representative confocal images of transcriptional
780 reporters for *PjRGF1* (*PjRGF1pro*), *PjRGF2* (*PjRGF2pro*), and *PjRGF5-5* (*PjRGF5pro*5) prior
781 to 10 µM treatment of DMBQ, 1 DPT 10 µM DMBQ, and 1 DPI. Both *PjRGF2pro* and
782 *PjRGF5pro* are localized to the prehaustorium while *PjRGF1pro* is not. C) Localization of
783 mNG-PjPLT after 1 DPT 10 µM DMBQ, 2 DPT 5 nM PjRGF2, and at 1 DPI. mNG-PjPLT
784 localizes within the prehaustorium of *P. japonicum* upon all treatments but the localization of
785 mNG-PjPLT slightly differs. Scale bars are 75 µm. Fluorescent Arabidopsis is expressing
786 *3SS::LT6-GFP*.
787
788 **Fig. 3. Genomic landscape of haustorium specific RGF peptides.** A) Illustration of the contigs
789 where *PjRGF5* duplications occur. Tandem duplications of *PjRGF5* occur on several contigs.
790 Only small sections of tig00008335_np1212 and tig00008333_np1212 are shown in the
791 illustration while the entirety of the other contigs are represented in the illustration. Blue *PjRGF5*
792 duplications encode viable genes and yellow *PjRGF5* duplications encode likely pseudogenes.
793 *PjRGF8* is shown in red. The short length of tig00008334_np1212, tig00000123_np1212, and

bioRxiv preprint doi: https://doi.org/10.1101/2025.02.09.637280; this version posted February 10, 2025. The copyright holder for this preprint (which was not certified by peer review) is the author/funder, who has granted bioRxiv a license to display the preprint in perpetuity. It is made available under a CC-BY-NC-ND 4.0 International license.

794 tig00000121_np1212 suggest a potentially complicated area of the genome to assemble. Colored
795 segments of each contig represent areas where Helitrons, TIRs, and LTRs occur. *PjRGF5-7*,
796 *PjRGF5-8*, and *PjRGF5-9* all have a TIR in the intron. B) Maximum-likelihood phylogenetic
797 tree with a Bootstrap of 100 made using identified and annotated RGF prepropeptides encoded in
798 the genomes of several species found in Orobanchaceae. Clades that include PjRGF1, PjRGF2,
799 and PjRGF5 are colored in pink, blue, and yellow, respectively. PjRGF1/2/5 are in bold. C)
800 Multiple sequence alignment of the C-terminus of the RGF prepropeptides found in clades with
801 PjRGF1/2/5. Only the PjRGF2 mature peptide sequence is conserved.
802
803 **Fig. 4. PjRGFR expression dynamics and their interactions with haustorium specific**
804 **PjRGFs.** A) Representative confocal images of transcriptional reporters for *PjRGFR1-6*
805 (*PjRGFRpro*) before treatment with 10 µM DMBQ, 1 DPT 10 µM DMBQ treatment, and at 1
806 DPI. The spatial expression pattern of *PjRGFR1/2/4/5* promoters at 1 DPI localize to the
807 prehaustorium. These expression patterns are less clear in roots at 1 DPT 10 µM DMBQ save for
808 the spatial expression pattern of *PjRGFR2pro*. At 1 DPT 10 µM DMBQ and 1 DPI, *PjRGFR2pro*
809 is expressed in the epidermal cells of the prehaustorium. Scale bars = 75 µm. Arabidopsis is
810 expressing *35S::LT6-GFP*. B,C) *PjRGFR-BRI1-HA* chimera and *BES1-HA* were expressed in *N.*
811 *benthamiana*. Treatment with B) 100 nM PjRGF2 resulted in dephosphorylation of BES1-HA
812 when PjRGFR1/3/4-BRI1-HA were expressed and with C) 100 nM PjRGF5 resulted in
813 dephosphorylation of BES1-HA when PjRGFR3/4-BRI-HA were expressed.
814
815 **Fig. 5. PjRGF signaling pathway is necessary for prehaustorium induction.** A) Microscopic
816 images of *P. japonicum* hairy roots overexpressing RUBY exhibited four distinct phenotypes

bioRxiv preprint doi: https://doi.org/10.1101/2025.02.09.637280; this version posted February 10, 2025. The copyright holder for this preprint (which was not certified by peer review) is the author/funder, who has granted bioRxiv a license to display the preprint in perpetuity. It is made available under a CC-BY-NC-ND 4.0 International license.

following 10 µM DMBQ treatment. These phenotypes were characterized as no prehaustorium, some cell division occurred (scored as no prehaustorium), prehaustorium, prehaustorium with aberrant cell division, and aborted prehaustorium. Roots that exhibited some cell division were characterized as having no prehaustorium. Cell division can be seen to be occurring in the area in between the dotted lines in the representative photo for roots with some cell division. Scale bar = 200 µm B) Graph showing the percent of *P. japonicum* hairy roots exhibiting the previously described phenotypes. *PjRGF2* KO, *PjRGFR1* KO, and *PjRGFR3* KO hairy roots showed a significant difference in normal prehaustorium development as compared to control hairy roots while *PjRGFR4* KO hairy roots did not show a significant difference in prehaustorium development. p-values were calculated using a Mann-Whitney U test.

bioRxiv preprint doi: https://doi.org/10.1101/2025.02.09.637280; this version posted February 10, 2025. The copyright holder for this preprint (which was not certified by peer review) is the author/funder, who has granted bioRxiv a license to display the preprint in perpetuity. It is made available under a CC-BY-NC-ND 4.0 International license.

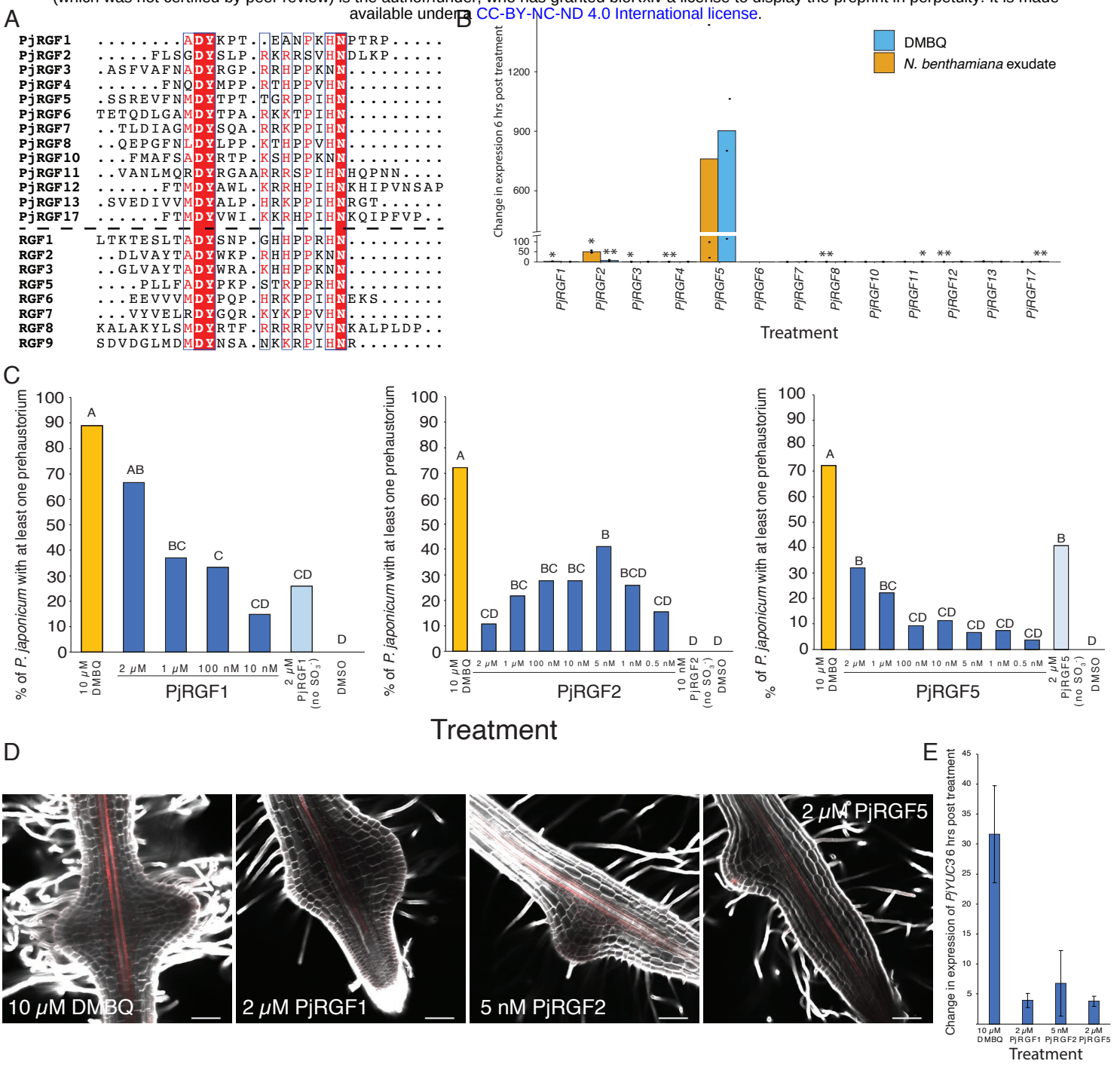


Fig. 1. PjRGF peptides induce prehaustoria. A) Multiple sequence alignment of the C-terminus of the identified RGF peptides in *P. japonicum* and eight of the eleven RGF peptides in Arabidopsis. B) Change in expression of the identified PjRGF peptides six hours post 10 μM DMBQ treatment or *N. benthamiana* treatment as compared to treatment with DMSO. Each dot represents the fold-change per biological replicate. *PjRGF5* was consistently up-regulated however the high-variability between replicates caused the p-value to be > 0.1. Student's T-test was used to determine statistical significance. * represents p-value < 0.05 **represents p-value < 0.1. C) Percent of *P. japonicum* forming at least one prehaustorium two day post treatment with DMBQ, PjRGF1, PjRGF2, or PjRGF5. One-way ANOVA followed by Tukey HSD was used for identifying statistical significance. D) Confocal images of P. japonicum two days after treatment with 10 μM DMBQ, 2 μM PjRGF1, 5 nM PjRGF2, or 2 μM PjRGF5 stained with calcofluor white (white) and basic fuschin (red). Scale bars = 75 μm. E) Change in expression of *PjYUC3* six hours post treatment with 10 μM DMBQ, 2 μM PjRGF1, 5 nM PjRGF2, or 2 μM PjRGF5.

(which was not certified by peer review) is the author/funder, who has granted bioRxiv a license to display the preprint in perpetuity. It is made available under a CC-BY-NC-ND 4.0 International license.

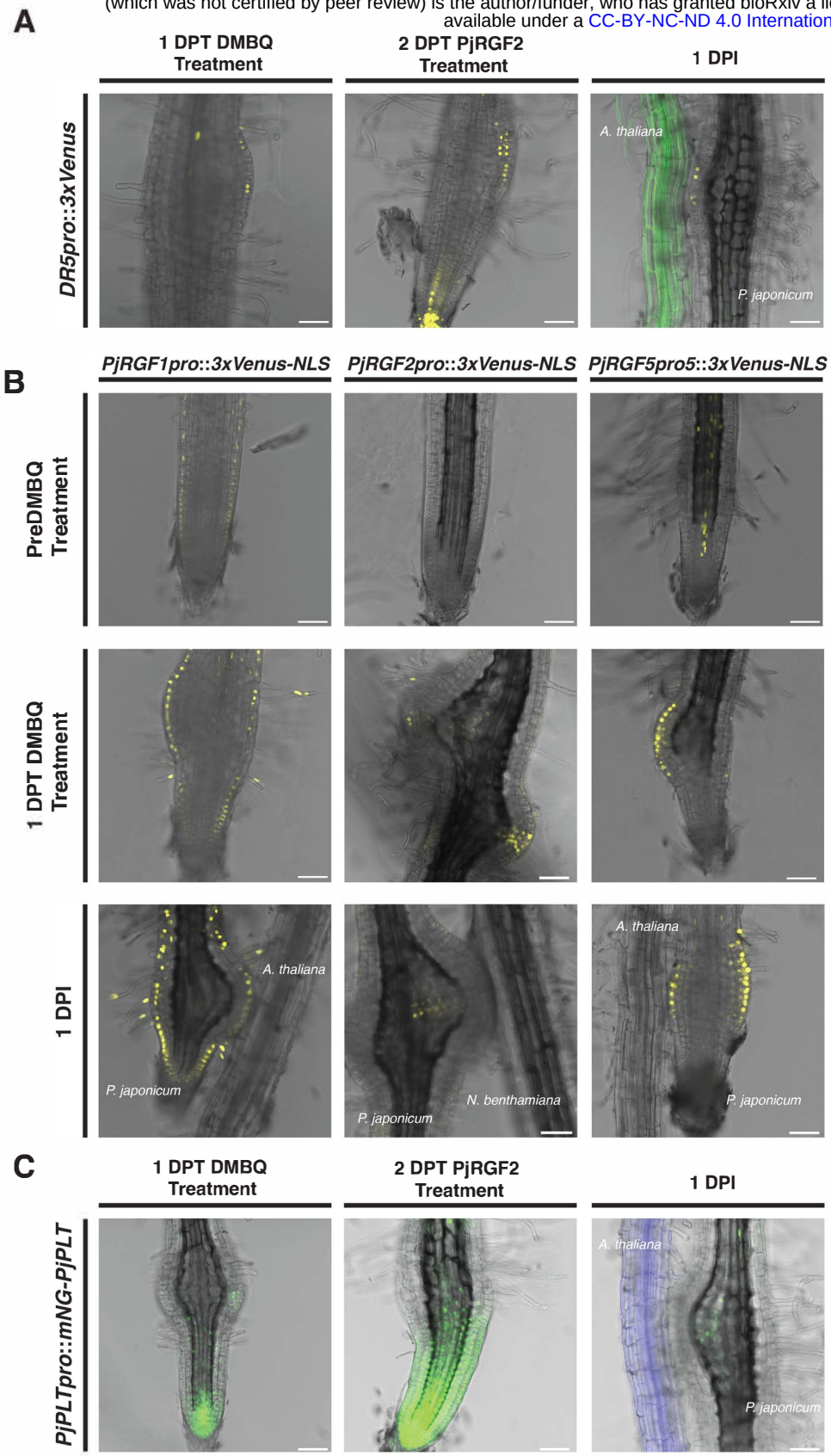
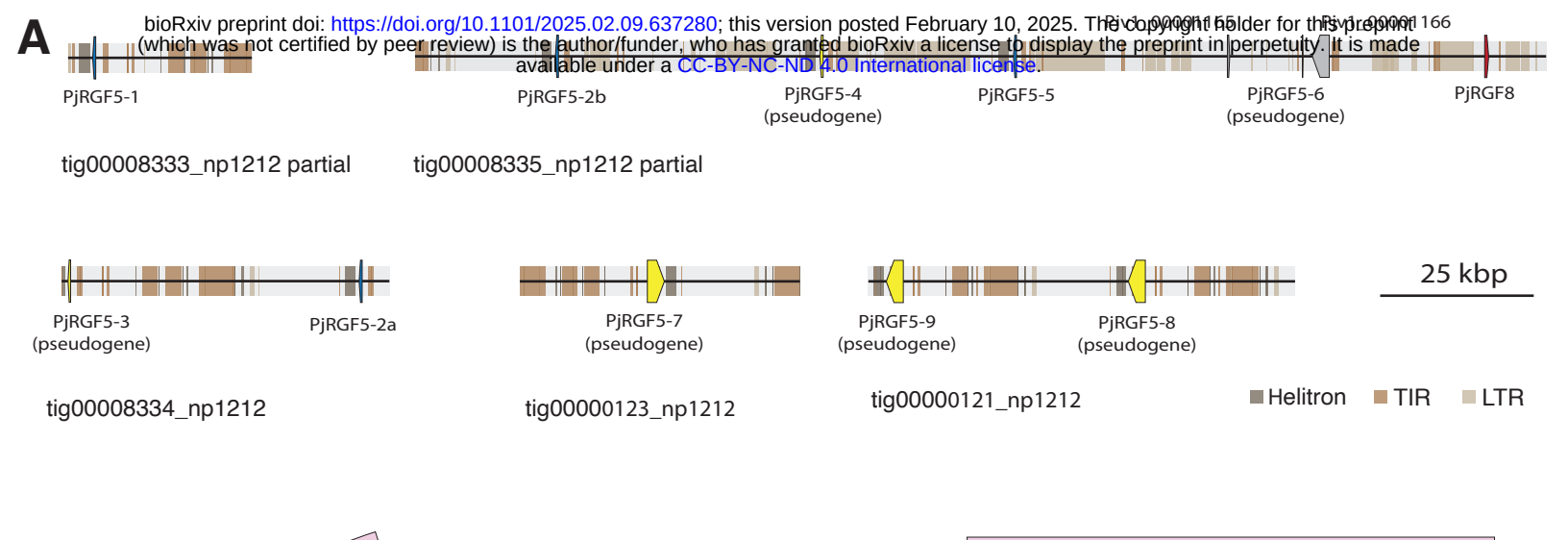
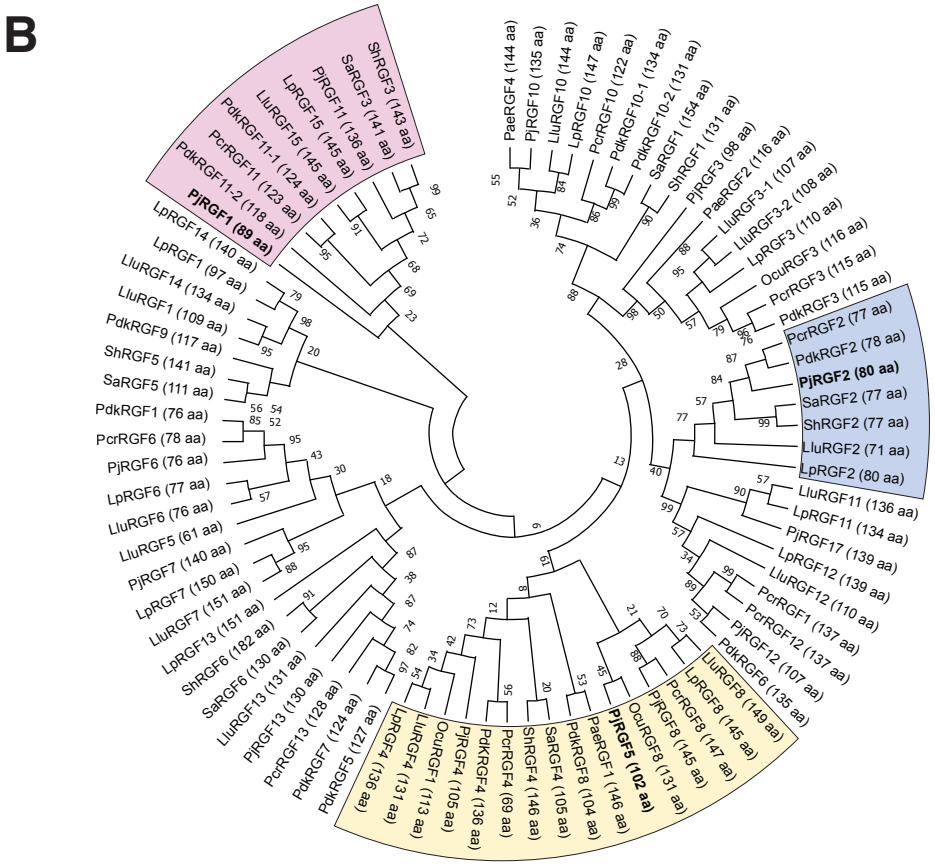


Fig. 2. Haustorial expression dynamics of PjRGF peptides and downstream signaling events. A) Expression of *3x-Venus-NLS* driven by the *DR5* promoter following 1 day post treatment (DPT) 10 μM DMBQ, 2 DPT 5 nM PjRGF2, and at 1 day post infection (DPI). *DR5* expression, which correlates with auxin localization, occurs at the epidermal cells at the apex of the prehaustorium in all treatments. B) Representative confocal images of transcriptional reporters for *PjRGF1 (PjRGF1pro), PjRGF2 (PjRGF2pro),* and *PjRGF5-5 (PjRG5pro5)* prior to 10 μM treatment of DMBQ, 1 DPT 10 μM DMBQ, and 1 DPI. Both *PjRGF2pro* and *PjRGF5pro5* are localized to the prehaustorium while *PjRGF1pro* is not. C) Localization of mNG-PjPLT after 1 DPT 10 μM DMBQ, 2 DPT 5 nM PjRGF2, and at 1 DPI. mNG-PjPLT localizes within the prehaustorium of *P. japonicum* upon all treatments but the localization of mNG-PjPLT slightly differs. Scale bars are 75 μm. Fluorescent Arabidopsis is expressing *3SS::LT6-GFP.*

bioRxiv preprint doi: https://doi.org/10.1101/2025.02.09.637280; this version posted February 10, 2025. The copyright holder for this preprint (which was not certified by peer review) is the author/funder, who has granted bioRxiv a license to display the preprint in perpetuity. It is made available under a CC-BY-NC-ND 4.0 International license.





Pj - *Phtheirospermum japonicum*
Pdk - *Pedicularis kansuensis*
Pcr - *Pedicularis cranolopha*
Ocu - *Orobanche cumana*
Pae - *Phelipanche aegyptiaca*
Lp- *Lindenbergia philippensis*
Llu- *Lindenbergia luchenensis*
Sh - *Striga hermonthica*
Sa - *Striga asiatica*

C

	1									10										20
Consensus	L	M	.	.	D	Y	.	G	.	.	R	R	.	.	P	I	.	N	.	E	P	.	N
PjRGF1	V	E	L	A	D	Y	K	.	.	P	T	E	A	N	P	K	H	N	P	T	R	P	.
PjRGF11	L	M	Q	R	D	Y	R	G	A	A	R	R	R	S	P	I	H	N	H	Q	P	N	N
PcrRGF11	L	M	Q	R	D	Y	K	G	A	A	R	R	R	S	P	I	H	N	Q	E	P	N	N
PdkRGF11-1	L	M	Q	R	D	Y	K	G	A	A	R	R	R	S	P	I	H	N	Q	E	P	N	N
PdkRGF11-2	L	M	Q	R	D	Y	K	G	A	A	R	R	R	S	P	I	H	N	Q	E	P	N	N
ShRGF3	L	M	R	R	D	Y	K	G	K	P	R	R	K	P	P	I	N	N	R	E	P	K	N
SaRGF3	L	M	R	R	D	Y	K	G	K	P	R	R	K	P	P	I	N	N	R	E	P	K	N
LluRGF15	L	M	R	K	D	Y	R	G	A	P	R	R	K	P	P	I	N	N	H	Q	P	K	N
LpRGF15	L	M	R	K	D	Y	R	G	A	P	R	R	K	P	P	I	N	N	H	Q	P	K	N

	1									10										20
Consensus	F	L	S	E	D	Y	S	L	P	R	K	R	.	.	V	.	N	.	L	.	P
PjRGF2	F	L	S	G	D	Y	S	L	P	R	K	R	R	S	V	H	N	D	L	K	P
PcrRGF2	F	M	S	E	D	Y	S	L	P	K	K	R	R	S	V	H	N	D	L	K	P
PdkRGF2	F	L	S	G	D	Y	S	L	P	R	K	R	R	S	V	H	N	D	L	K	P
SaRGF2	F	L	S	E	D	Y	S	L	P	R	K	R	Q	P	V	N	N	E	L	E	H
ShRGF2	F	L	S	E	D	Y	S	L	P	R	K	R	Q	P	V	N	N	E	L	E	H
LluRGF2	L	L	T	E	D	Y	T	L	P	R	R	R	Q	P	V	N	N	N	F	Q	P
LpRGF2	L	L	T	E	D	Y	T	L	P	R	R	R	Q	P	V	N	N	N	L	Q	P

	1									10										
Consensus	.	F	N	.	L	D	Y	L	P	P	.	T	H	P	P	V	H	N		
PjRGF5	V	F	N	.	M	D	Y	T	P	T	T	G	R	P	P	I	H	N		
PjRGF4	E	F	N	.	Q	D	Y	M	P	P	R	T	H	P	P	V	H	N		
PjRGF8	G	F	N	.	L	D	Y	L	P	P	K	T	H	P	P	V	H	N		
PcrRGF4	E	F	N	.	Q	D	Y	L	P	P	R	T	H	P	P	V	H	N		
PcrRGF8	E	F	N	.	L	D	Y	L	P	P	K	T	H	P	P	V	H	N		
PdkRGF4	E	F	N	.	Q	D	Y	L	P	P	R	T	H	P	P	I	H	N		
PdkRGF8	E	F	N	.	L	D	Y	F	P	P	K	T	H	P	P	T	H	N		
ShRGF4	G	F	N	.	L	D	Y	L	P	P	K	T	H	P	G	I	H	N		
SaRGF4	G	F	N	.	L	D	Y	L	P	P	K	T	H	P	G	I	H	N		
PaeRGF1	R	F	N	.	L	D	Y	L	P	P	K	T	H	P	P	A	H	N		
OcuRGF1	I	L	D	.	L	D	Y	V	P	P	R	T	H	P	P	V	H	N		
OcuRGF8	E	F	N	.	L	D	Y	L	P	P	R	T	H	P	P	S	H	N		
LluRGF4	G	F	N	N	L	D	Y	L	P	P	R	T	H	P	P	V	H	N		
LluRGF8	G	F	N	.	L	D	Y	L	P	P	K	T	H	P	P	V	H	N		
LpRGF4	G	F	N	D	L	D	Y	L	P	P	R	T	H	P	P	V	H	N		
LpRGF8	G	F	N	.	L	D	Y	L	P	P	K	T	H	P	P	V	H	N		

Fig. 3. Genomic landscape of haustorium specific RGF peptides. A) Illustration of the contigs where *PjRGF5* duplications occur. Tandem duplications of PjRGF5 occur on several contigs. Only small sections of tig00008335_np1212 and tig00008333_np1212 are shown in the illustration while the entirety of the other contigs are represented in the illustration. Blue *PjRGF5* duplications encode viable genes and yellow *PjRGF5* duplications encode likely pseudogenes. *PjRGF8* is shown in red. The short length of tig00008334_np1212, tig00000123_np1212, and tig00000121_np1212 suggest a potentially complicated area of the genome to assemble. Colored segments of each contig represent areas where Helitrons, TIRs, and LTRs occur. *PjRGF5-7*, *PjRGF5-8*, and *PjRGF5-9* all have a TIR in the intron. B) Maximum-likelihood phylogenetic tree with a Bootstrap of 100 made using identified and annotated RGF prepropeptides encoded in the genomes of several species found in Orobanchaceae. Clades that include PjRGF1, PjRGF2, and PjRGF5 are colored in pink, blue, and yellow, respectively. PjRGF1/2/5 are in bold. C) Multiple sequence alignment of the C-terminus of the RGF prepropeptides found in clades with PjRGF1/2/5. Only the PjRGF2 mature peptide sequence is conserved.

bioRxiv preprint doi: https://doi.org/10.1101/2025.02.09.637280; this version posted February 10, 2025. The copyright holder for this preprint (which was not certified by peer review) is the author/funder, who has granted bioRxiv a license to display the preprint in perpetuity. It is made available under a CC-BY-NC-ND 4.0 International license.

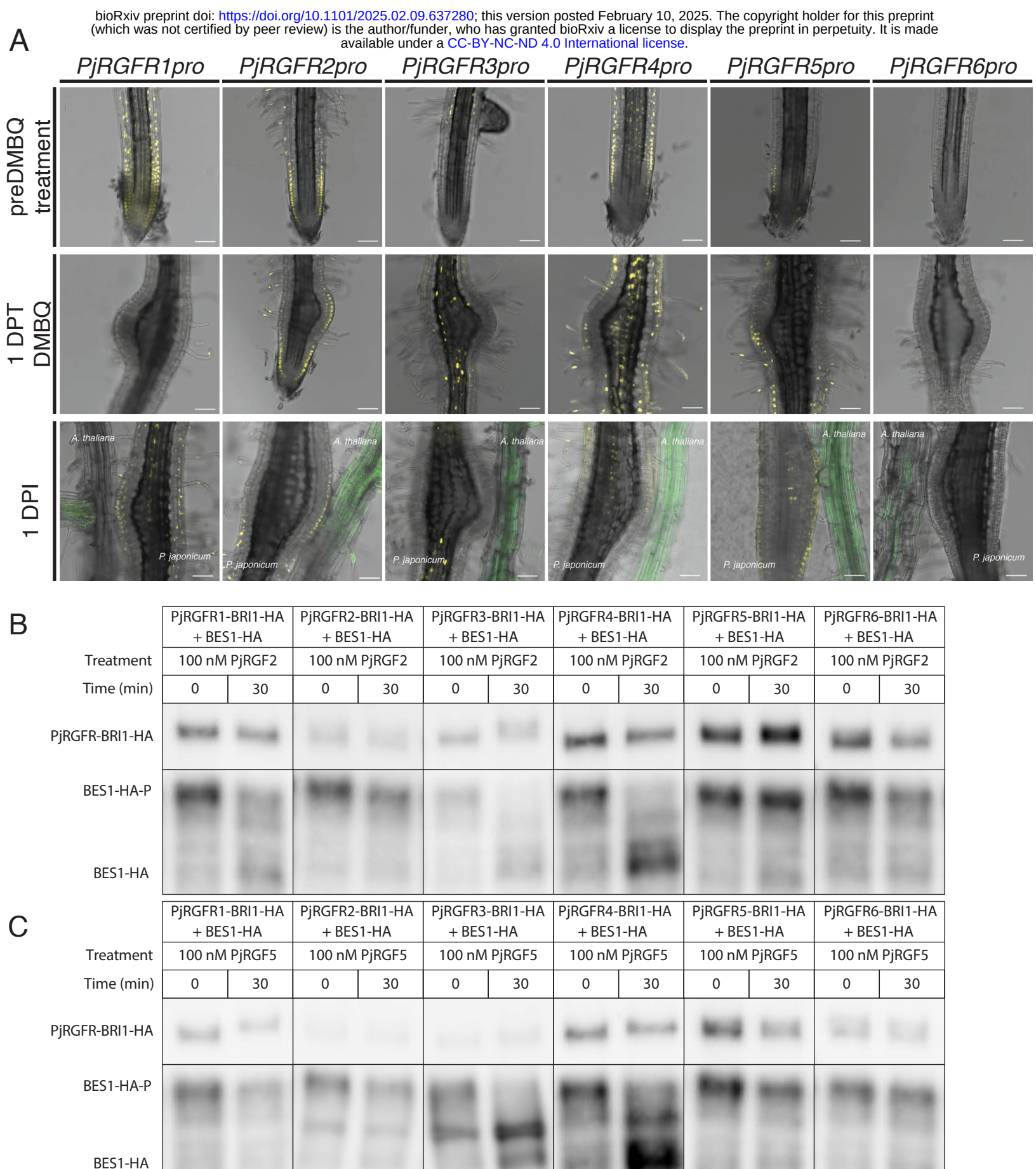


Fig. 4. PjRGFR expression dynamics and their interactions with haustorium specific PjRGFs. A) Representative confocal images of transcriptional reporters for *PjRGFR1-6* (*PjRGFRpro*) before treatment with 10 μM DMBQ, 1 DPT 10 μM DMBQ treatment, and at 1 DPI. The spatial expression pattern of *PjRGFR1/2/4/5 promoters* at 1 DPI localize to the prehaustorium. These expression patterns are less clear in roots at 1 DPT 10 μM DMBQ save for the spatial expression pattern of *PjRGFR2pro*. At 1 DPT 10 μM DMBQ and 1 DPI, PjRGFR2pro is expressed in the epidermal cells of the prehaustorium. Scale bars = 75 μm. Arabidopsis is expressing *35S::LT6-GFP*. B,C) PjRGFR-BRI1-HA chimera and BES1-HA were expressed in *N. benthamiana.* Treatment with B) 100 nM PjRGF2 resulted in dephosphorylation of BES1-HA when PjRGFR1/3/4-BRI1-HA were expressed and with C) 100 nM PjRGF5 resulted in dephosphorylation of BES1-HA when PjRGFR3/4-BRI-HA were expressed.

bioRxiv preprint doi: https://doi.org/10.1101/2025.02.09.637280; this version posted February 10, 2025. The copyright holder for this preprint (which was not certified by peer review) is the author/funder, who has granted bioRxiv a license to display the preprint in perpetuity. It is made available under a CC-BY-NC-ND 4.0 International license.

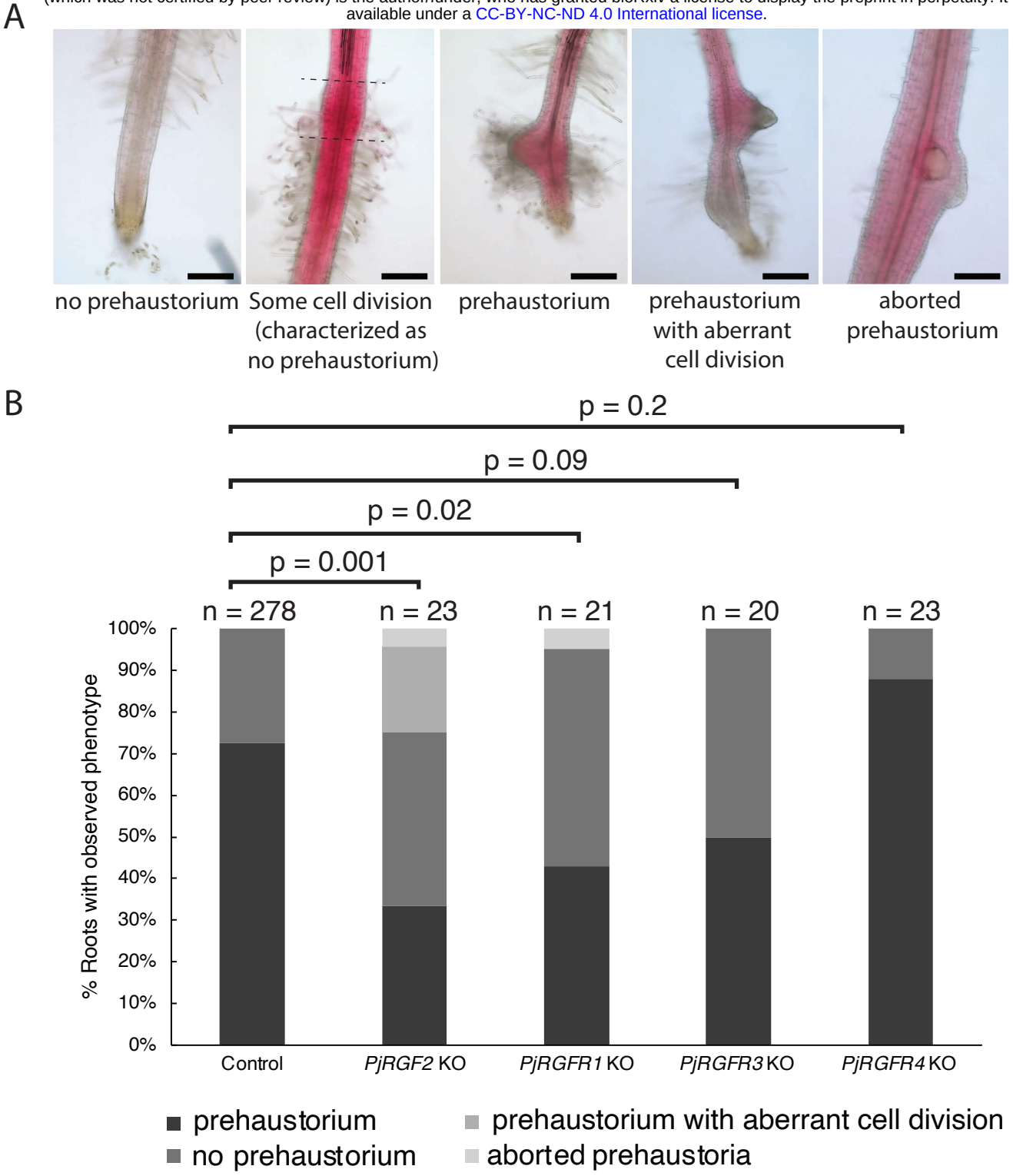


Fig. 5. PjRGF signaling pathway is necessary for prehaustorium induction. A) Microscopic images of *P. japonicum* hairy roots overexpressing RUBY exhibited four distinct phenotypes following 10 μM DMBQ treatment. These phenotypes were characterized as no prehaustorium, some cell division occurred (scored as no prehaustorium), prehaustorium, prehaustorium with aberrant cell division, and aborted prehaustorium. Roots that exhibited some cell division were characterized as having no prehaustorium. Cell division can be seen to be occurring in the area in between the dotted lines in the representative photo for roots with some cell division. Scale bar = 200 μm B) Graph showing the percent of *P. japonicum* hairy roots exhibiting the previously described phenotypes. *PjRGF2* KO, *PjRGFR1* KO, and PjRGFR3 KO hairy roots showed a significant difference in normal prehaustorium development as compared to control hairy roots while *PjRGFR4* KO hairy roots did not show a significant difference in prehaustorium development. p-values were calculated using a Mann-Whitney U test.